

Vibration isolation for the KAGRA beam splitter and signal recycling optics

FABIÁN PENA ARELLANO ON BEHALF OF THE KAGRA COLLABORATION
ICRR, THE UNIVERSITY OF TOKYO

Outline

- About KAGRA: cryogenic payload, underground location and types of suspensions.
- Description of the Type B suspension: mechanics.
- Type B suspension model prediction: control loop noise within the interferometer observation band.
- Future work
- Conclusions

Acknowledgment

- **Core Type B team:** Mark Barton (leader), Fabian Peña Arellano, Naoatsu Hirata.
- **Other VIS members:** Ryutaro Takahashi (VIS leader), Yoshinori Fujii, Yoichi Aso (manager), Koki Okutomi, Ayaka Shoda, Naoisha Sato, Hideharu Ishisaki, Lucia Trozzo.
- **Previous members:** Enzo Tapia San Martin, Takanori Sekiguchi, Naoko Ohishi, Daisuke Tatsumi, Riccardo De Salvo.
- **Others:** Raffaele Flaminio, Akutsu, Tomotada Akutsu, Simon Zeidler.
- **Students:** Yuhang Zhao, Kazuya Yokogawa, Yuya Kuwahara, Yingtang Liu, Toshiya Yoshioka, Perry Forsyth, Panwei Huang, Rikako Hatoya, Terrence Tsang, Ryohei Kozu.

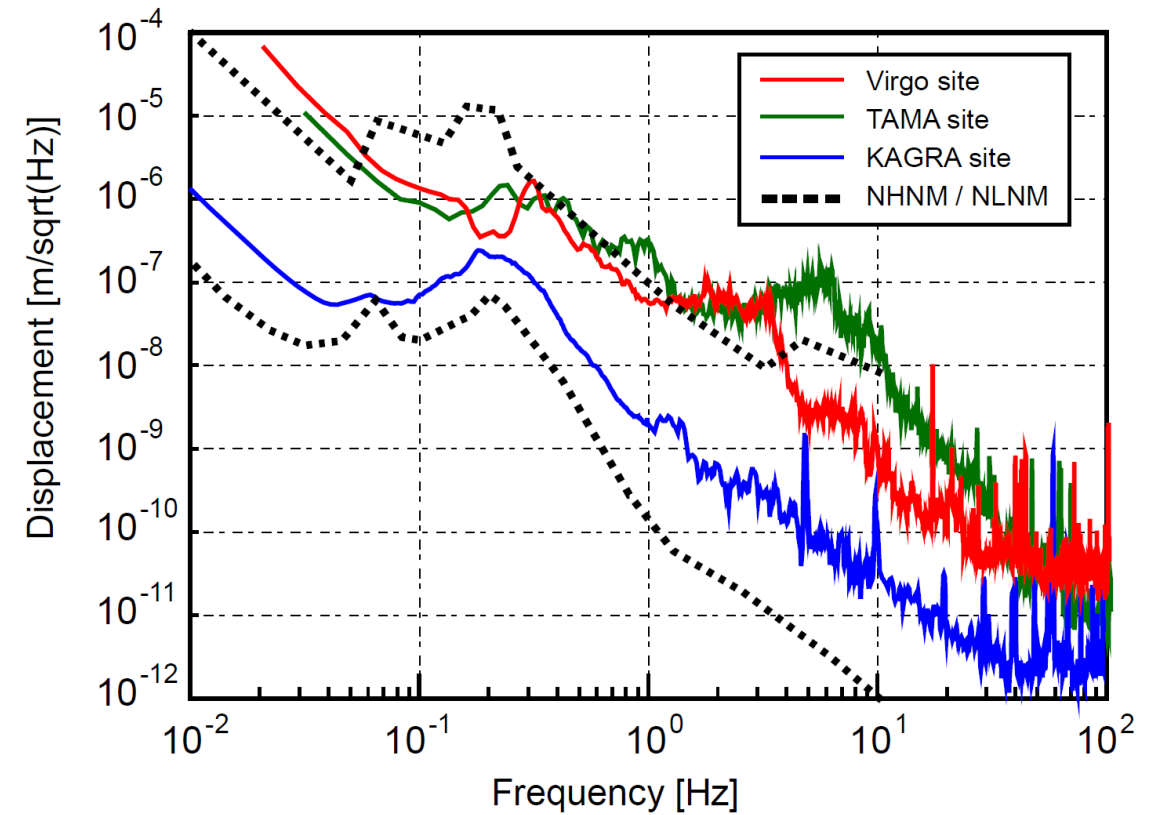
- Akiyama et al. “**Vibration isolation system with a compact damping system for power recycling mirrors of KAGRA.**” *Classical and Quantum Gravity*, 12 April 2019, **36** 095015.
- Fabián Peña Arellano et al. “**Characterization of the room temperature payload prototype for the cryogenic interferometric gravitational wave detector KAGRA.**” *Review of Scientific Instruments*, **87**, 034501 (2016).
- T. Sekiguchi, “**A study of low frequency vibration isolation system for large scale gravitational wave detectors,**” PhD thesis, University of Tokyo, 2016.
- K. Okutomi, “**Development of a 13.5-meter-tall Vibration Isolation System for the Main Mirrors in KAGRA,**” PhD thesis, The Graduate University of Advances Studies, 2019.
- Mark Beker, “**Low frequency sensitivity of next generation gravitational wave detectors,**” PhD thesis, Nikhef, 2013.
- Matheus Blom, “**Seismic attenuation for Advanced Virgo: vibration isolation for the external injection bench,**” PhD thesis, Nikhef, 2015.
- Alexander Wanner, “**Seismic Attenuation System (AEI-SAS) for the AEI 10 m Prototype,**” PhD thesis, Leibniz Universität Hannover, 2013.

Introduction

WHAT KAGRA IS

KAGRA is an underground detector

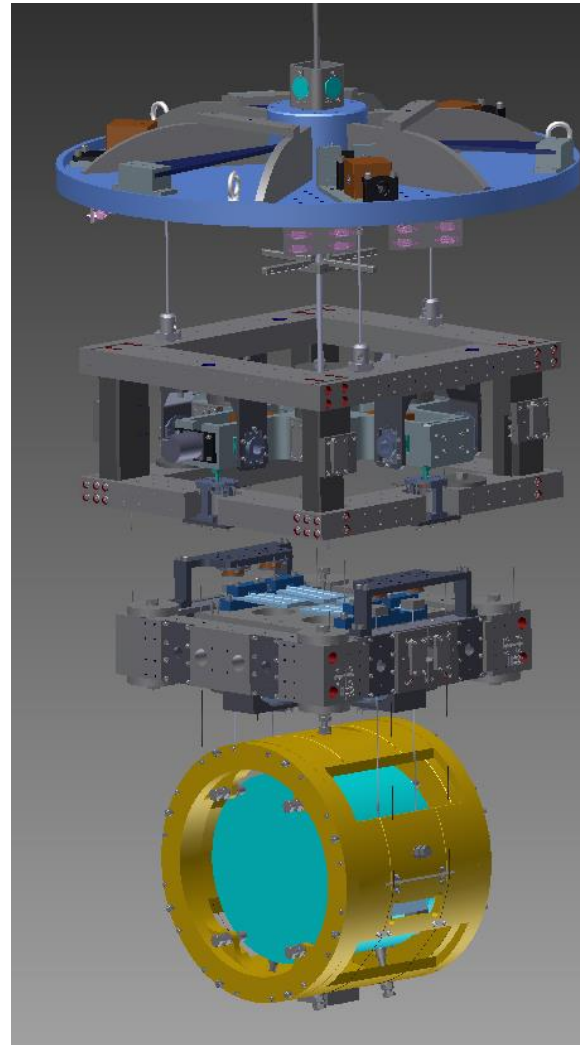
Depending in the frequency between 10 and 100 times reduction between TAMA and KAGRA sites



Plot by Takanori Sekiguchi

KAGRA is a cryogenic detector (1)

- Sapphire mirrors
- Cooled down to 20 K
- Mass of 200 kg



Drawing by A. Hawigara

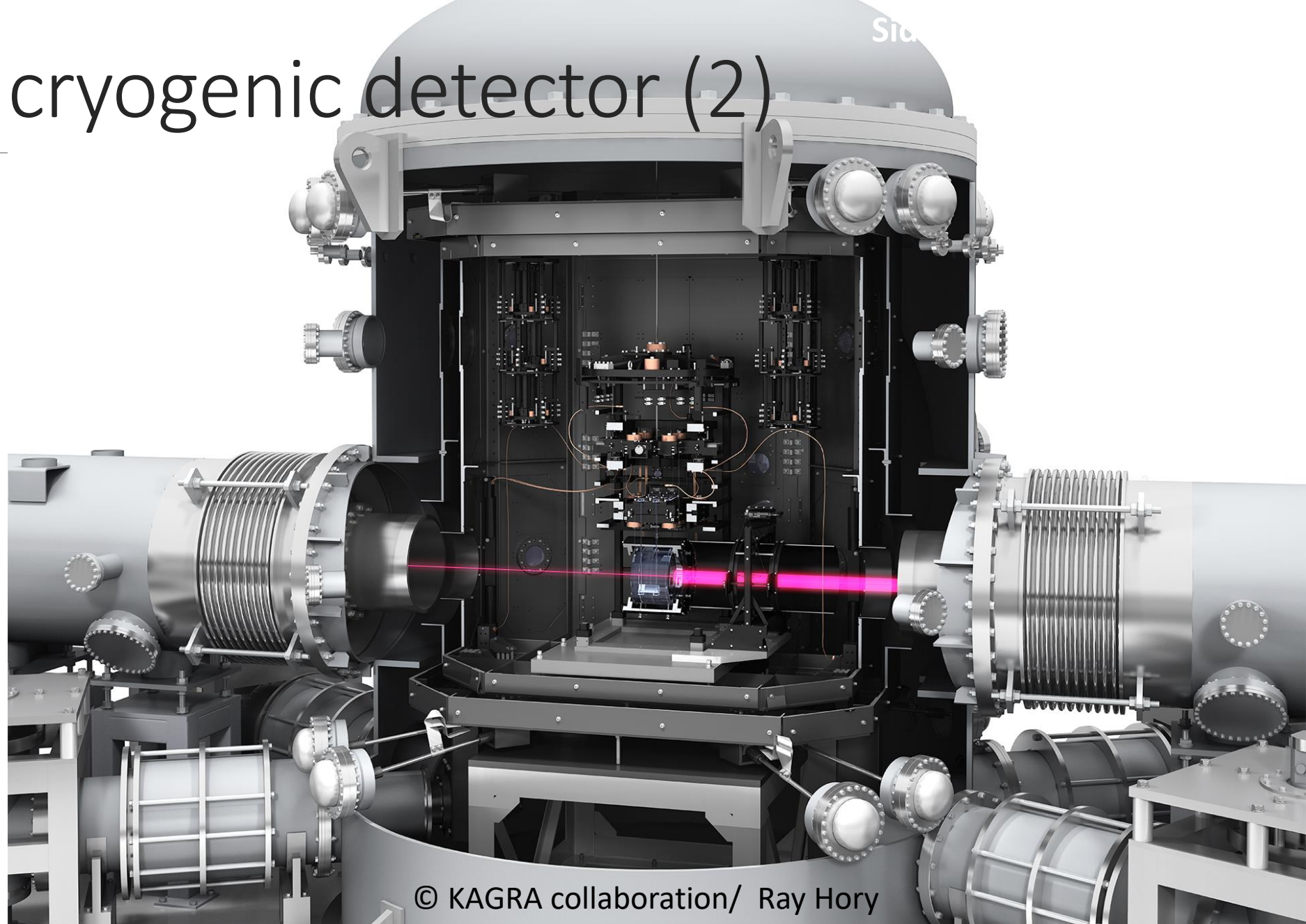


Photo by Tomotada Akutsu

Don't expect a tropical place like Natal!

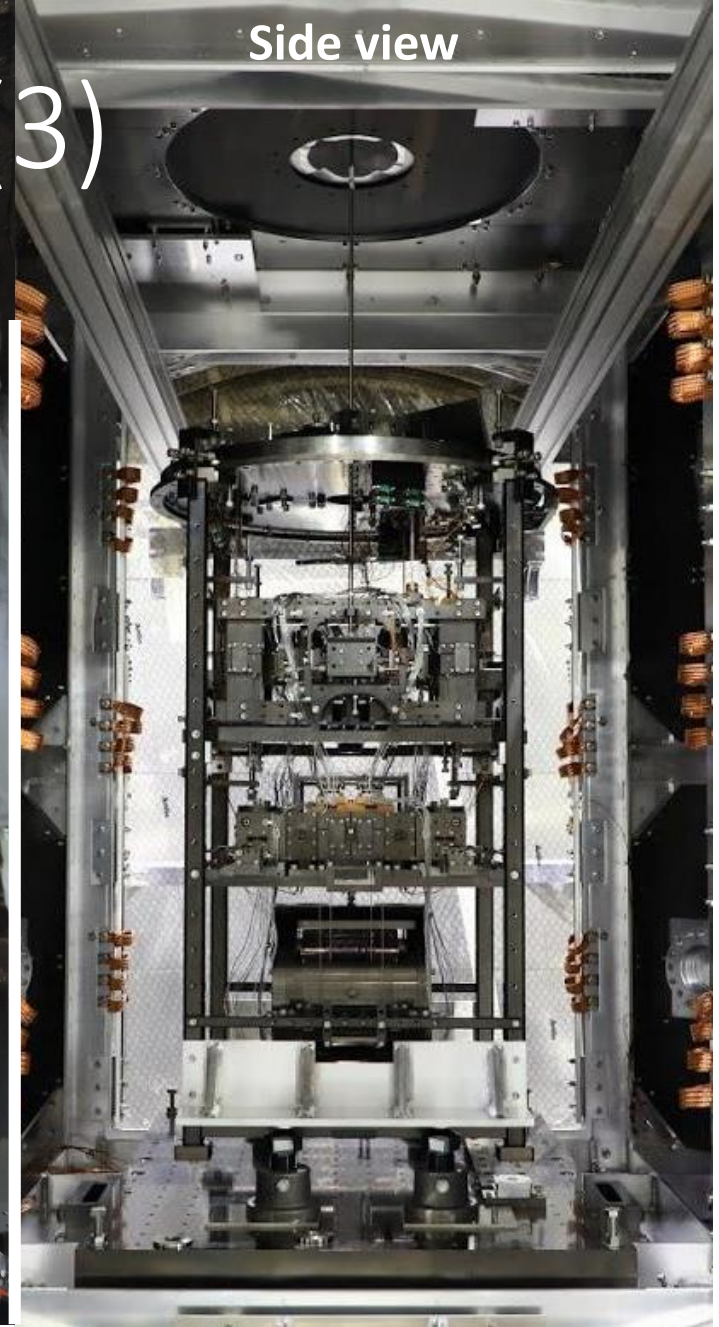
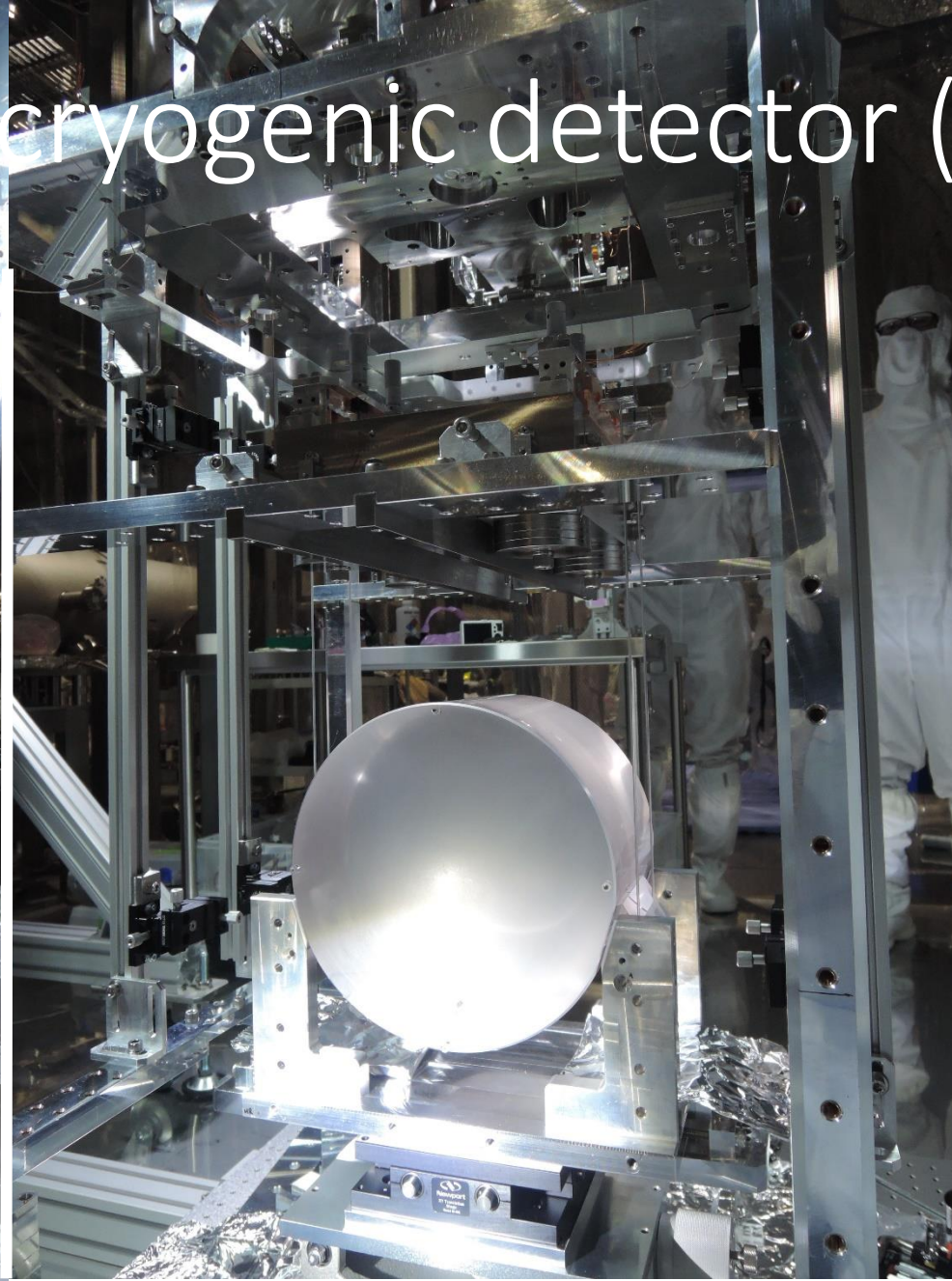
KAGRA is a cryogenic detector (2)

- Sapphire mirrors
- Cooled down to 20 K
- Mass of 200 kg



© KAGRA collaboration/ Ray Hory

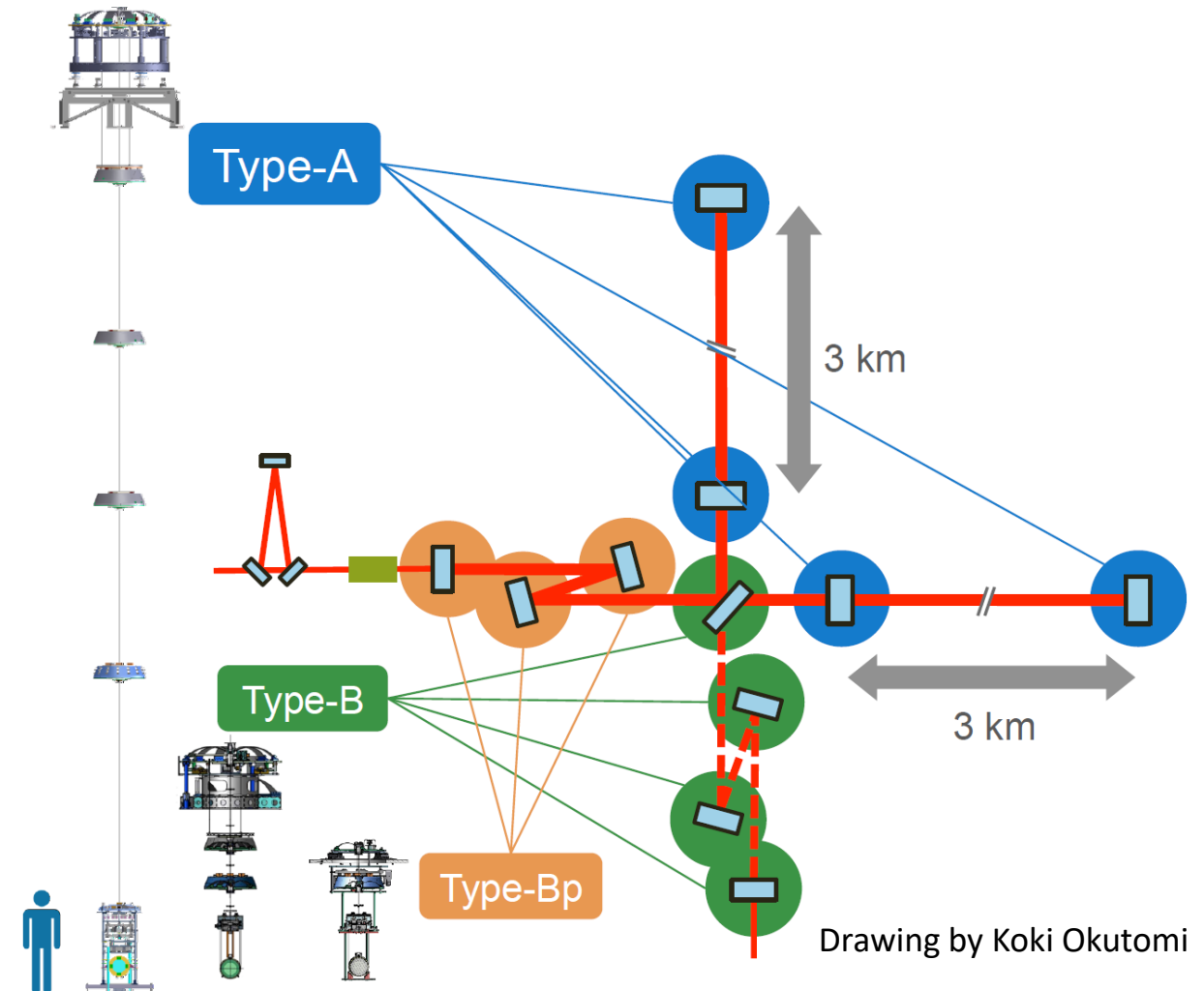
KAGRA is a cryogenic detector (3)



Photos: Rahul Kumar and Higiwara.

Suspensions for the main interferometer mirrors (1)

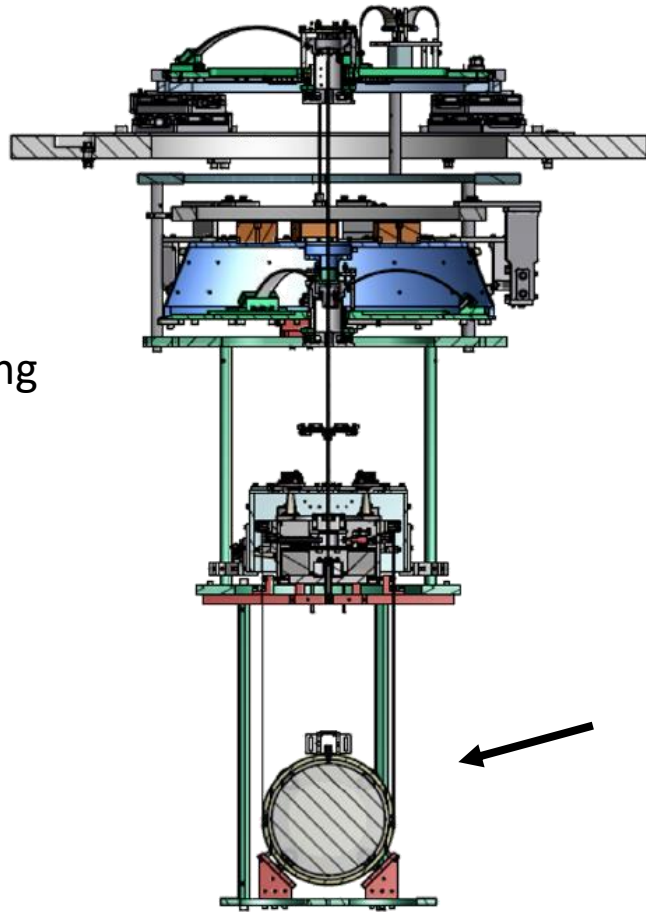
- 4 × Type A for the Test Masses sensitive to GW.
- 4 × Type B for the beam splitter and signal recycling mirrors.
- 3 × Type Bp for the power recycling mirrors.



Suspensions for the main interferometer mirrors (2)

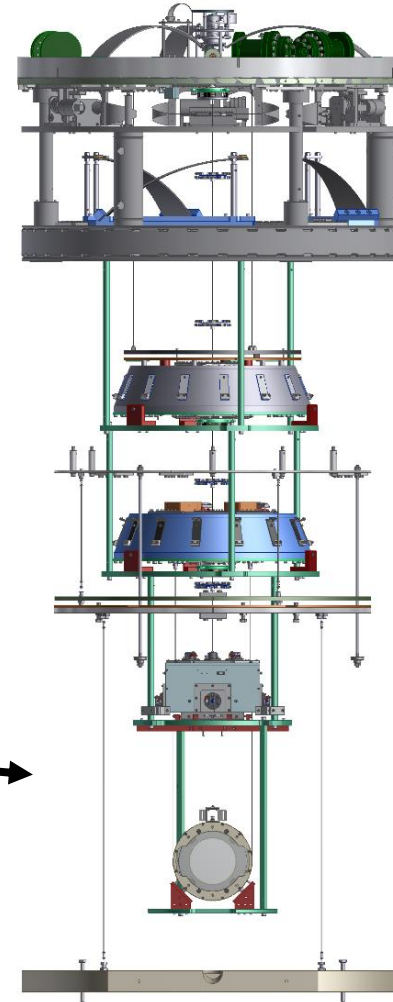
Type Bp

Power recycling mirrors



Type B

Beam splitter and signal recycling mirrors



Room temperature payload

Type A

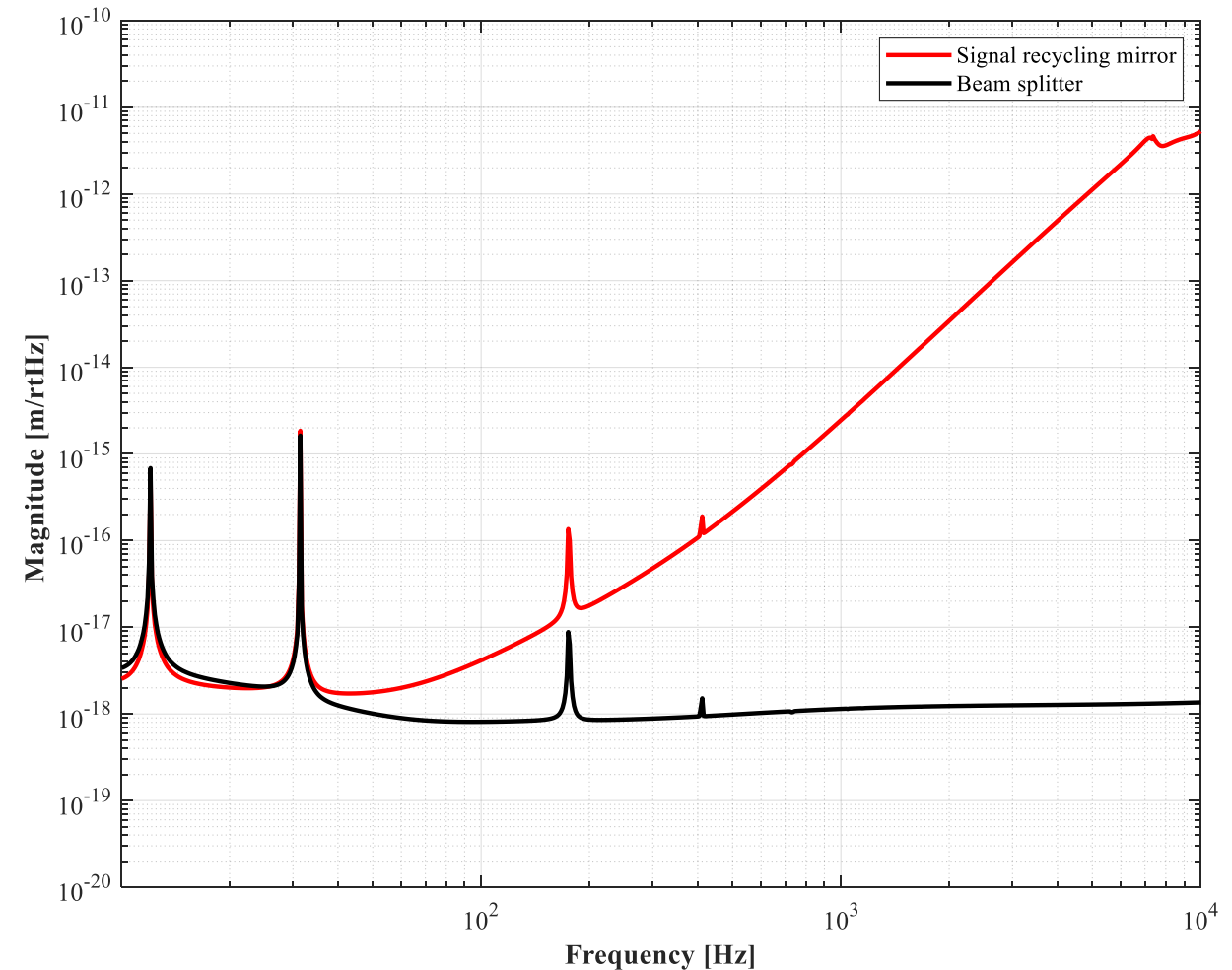
Test masses

Cryogenic payload



Aim of requirements

- At high frequencies above and at 10 Hz: to achieve the interferometer **target sensitivity**.
 - Beam splitter: 3.39×10^{-18} m/√Hz at 10 Hz.
 - Signal recycling mirror: 2.54×10^{-18} m/√Hz at 10 Hz.
- At low frequencies:
 - **Lock acquisition**: $v = 0.5$ μm/s (integrated RMS).
 - Interferometer **stable operation**: pitch and yaw **1 μm RMS** displacement.
 - **Quick recovery** after losing the interferometer lock (e.g. due to an earthquake): time constant upon damping of less than **60 seconds**.
 - Enzo Tapia will talk about the performance at low frequencies.



Passive vibration isolation

A simple example:

$$M\ddot{x} = -k(x - x_0)$$

x : position of the load.

x_0 : position of the ground.

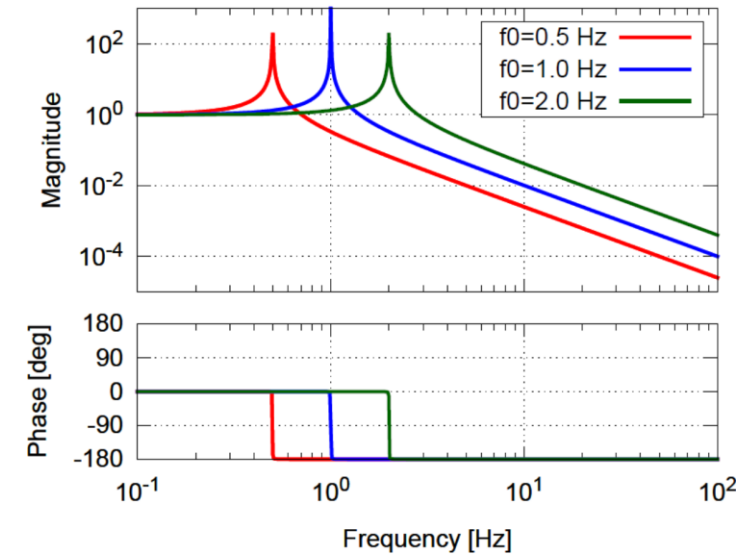
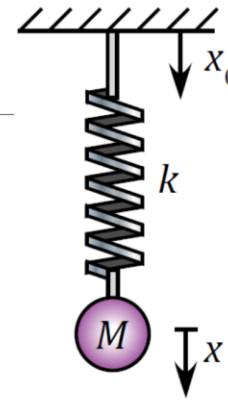
M : mass of the load.

k : stiffness of the spring.

$$\omega_0 = \sqrt{\frac{k}{M}}$$

The solution in frequency domain yields the **transfer function**:

$$H(\omega) \equiv \frac{\tilde{x}(\omega)}{\tilde{x}_0(\omega)} = \frac{1}{1 - (\omega/\omega_0)^2}$$



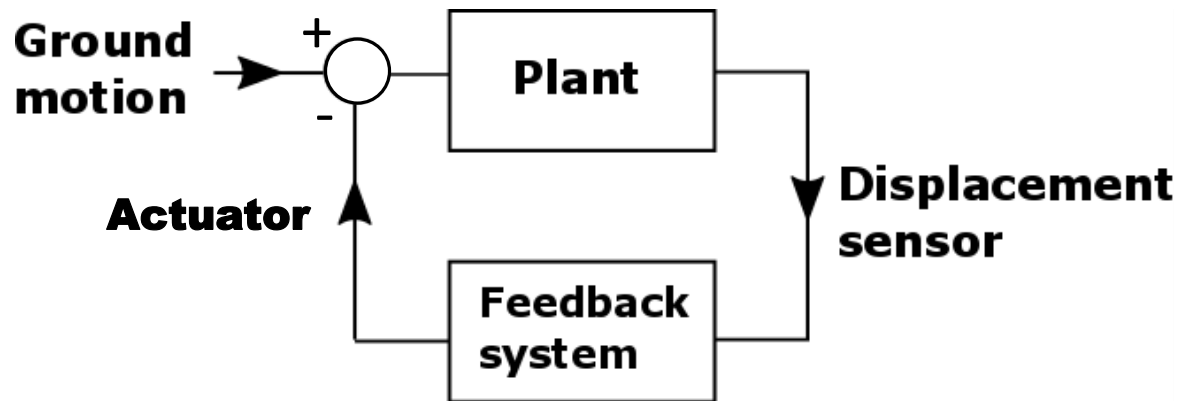
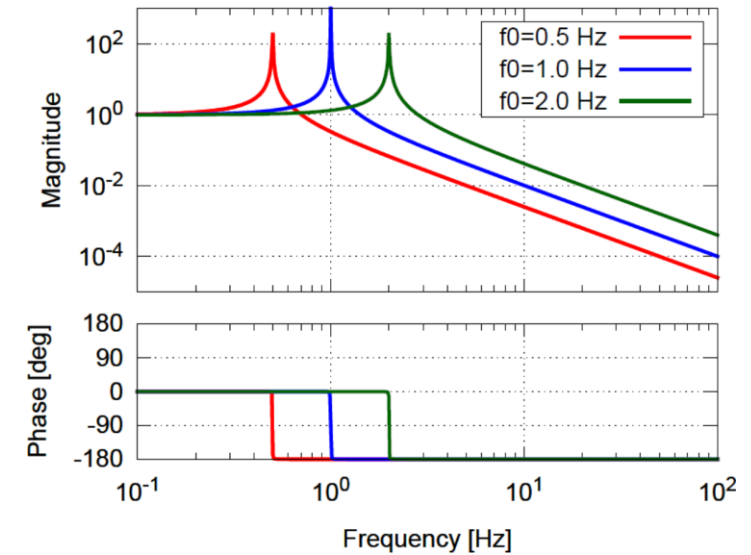
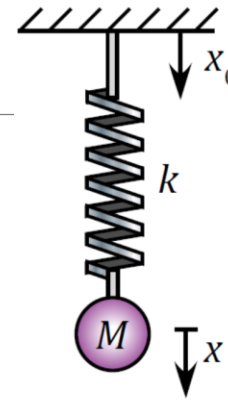
Above the resonant frequency the vibrations are filtered.

Challenge: support a heavy load (100s of kg) with a very soft system (low resonant frequency).

T. Sekiguchi, "A study of low frequency vibration isolation system for large scale gravitational wave detectors," Ph.D. thesis, University of Tokyo, 2016.

Active vibration isolation

- The system still has resonant movement that has to be damped
- We need to damp resonant motion to keep stability of the optical system.

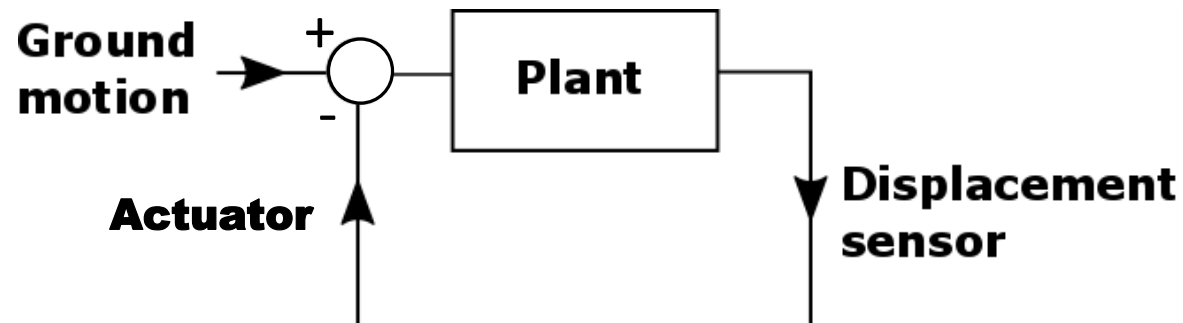


- Geophones for velocity.
- Shadow sensors for displacement.
- Inductive sensors for displacement.

T. Sekiguchi, "A study of low frequency vibration isolation system for large scale gravitational wave detectors," Ph.D. thesis, University of Tokyo, 2016.

Transfer functions

- Other type of transfer functions are measured with the control loop open.
- We move the system according to a prescription and sense its response.



We use them for

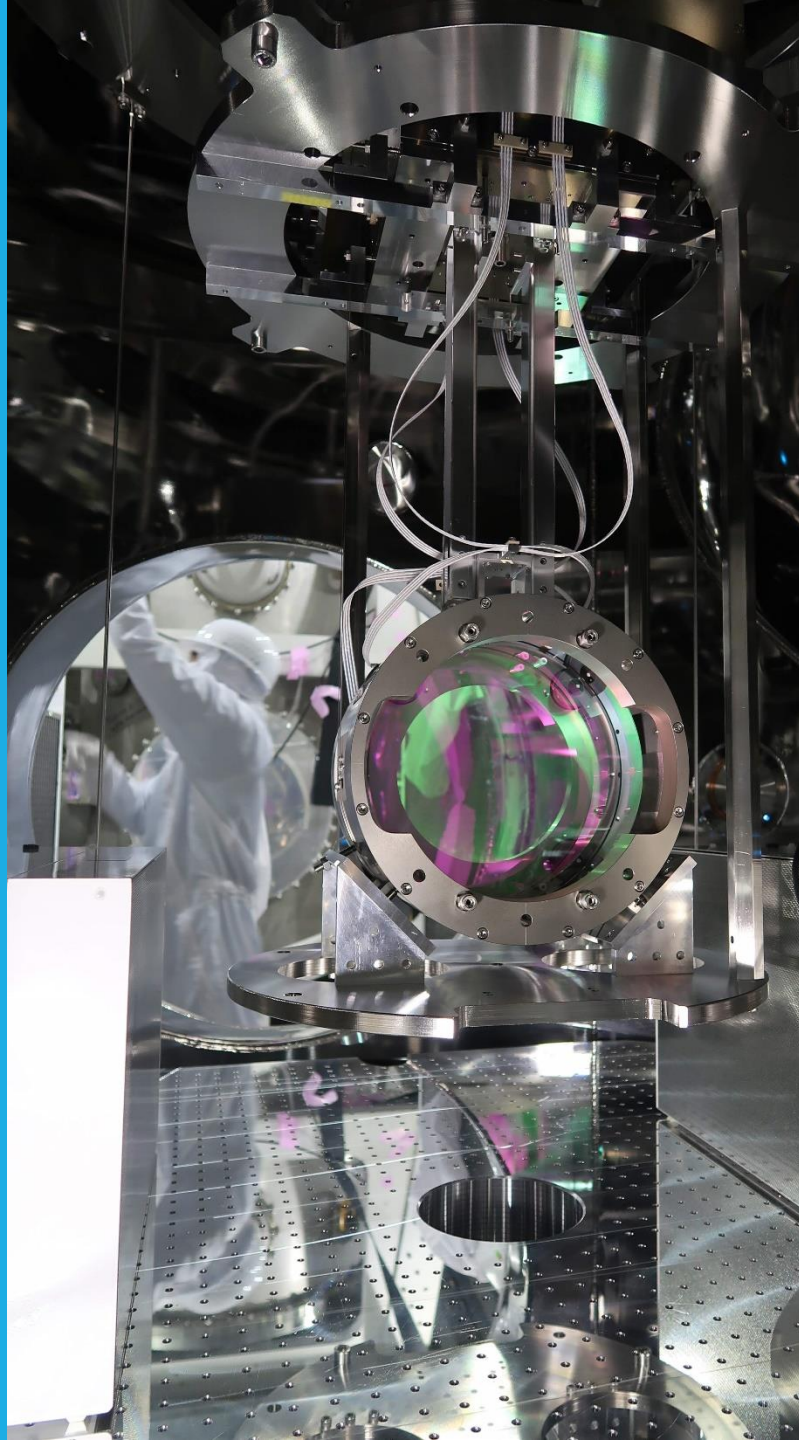
- Assessing the health of the system
 - Otherwise freely hanging components are touching each other.
 - Misconnected or disconnected cables
 - Errors in the software
- Designing controls filters offline.

Description of the Type B suspension

Room temperature

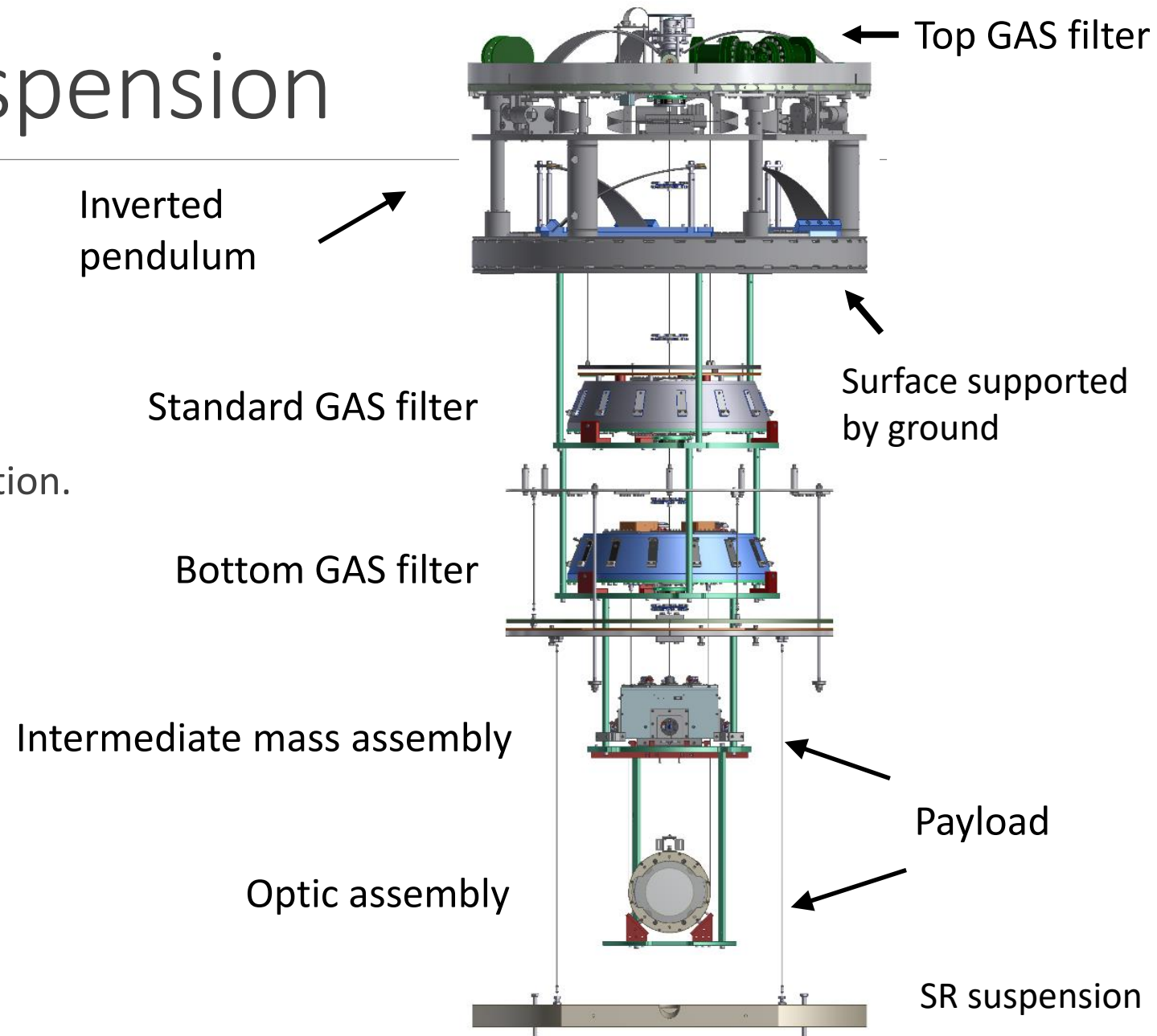
Beam splitter

Three signal recycling mirrors



Overview of the suspension

- Quadruple pendulum.
- A pre-isolator:
 - Inverted pendulum horizontal isolation.
 - GAS filter for vertical isolation.
- A chain with 3 × GAS filters for vertical isolation.
- Magnetic damper.
- Payload:
 - Marionette and its recoil body.
 - Optic and its recoil body.
- Sensors and actuators.
- Optical lever.
- Suspended optical table.



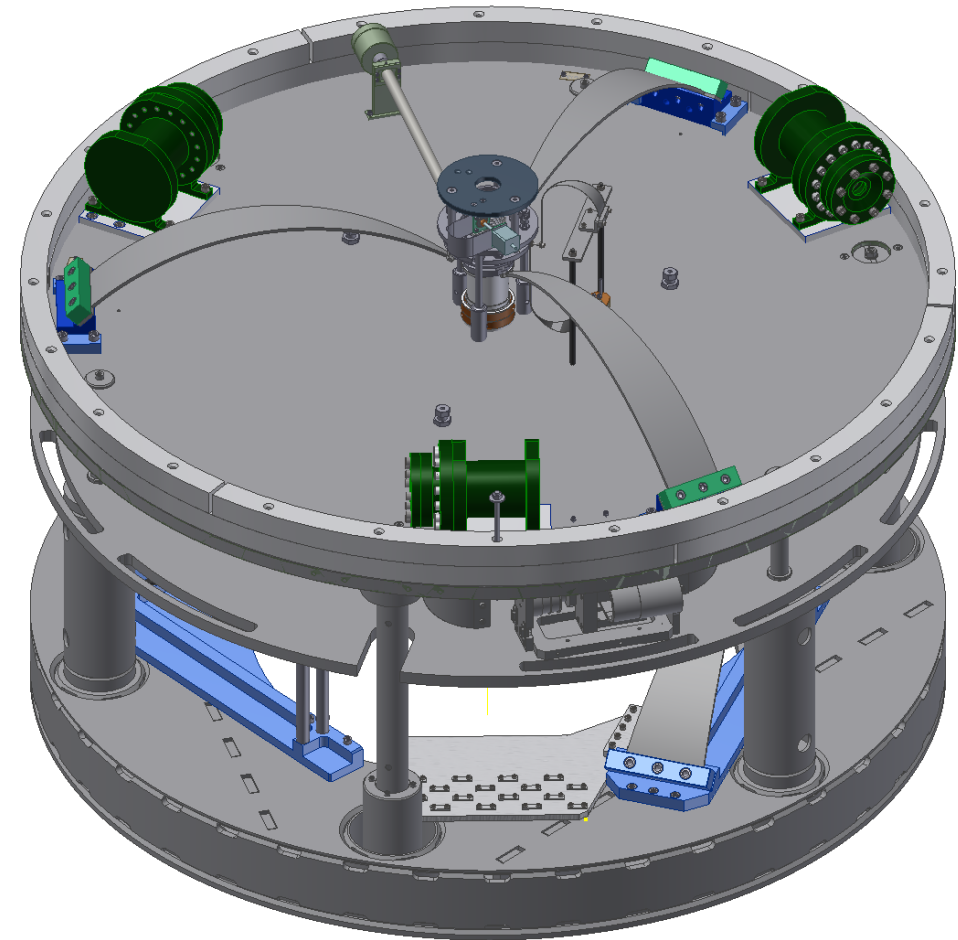
Basic elements of the pre-isolator

Inverted pendulum for horizontal isolation

- 3 × IP legs
- 3 × Geophones for inertial damping.
- 3 × LVDTs for position measurement.
- 3 × Coil-magnet actuators.
- 3 × Horizontal mechanical actuators.

Geometric anti-spring filter for vertical isolation

- Three maraging steel blades.
- 1 × LVDT for position measurement.
- 1 × Coil-magnet actuator.
- 1 × Vertical mechanical actuator (fishing rod).
- 1 × Yaw mechanical actuator.

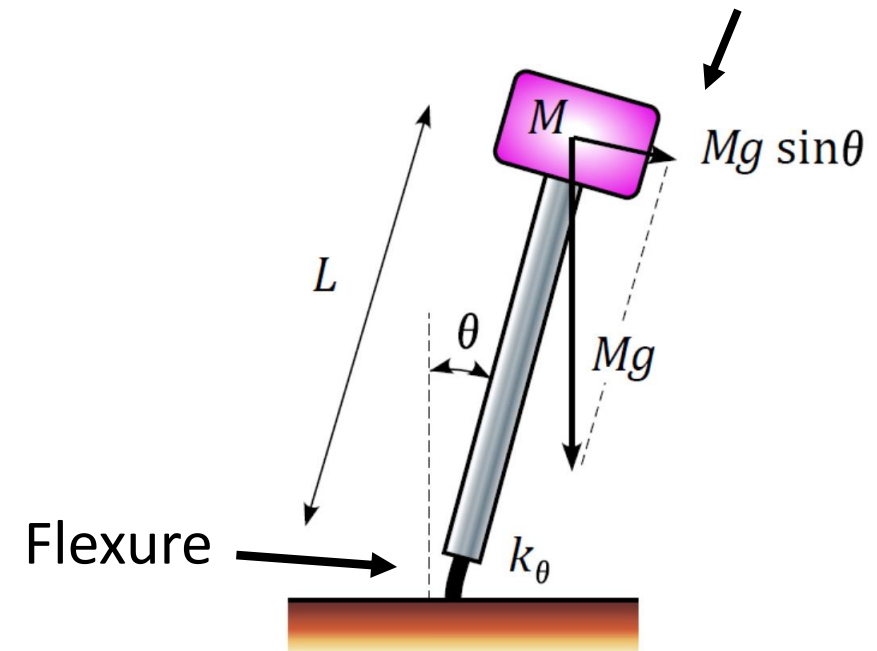


SR pre-isolator

Inverted pendulum: horizontal isolation

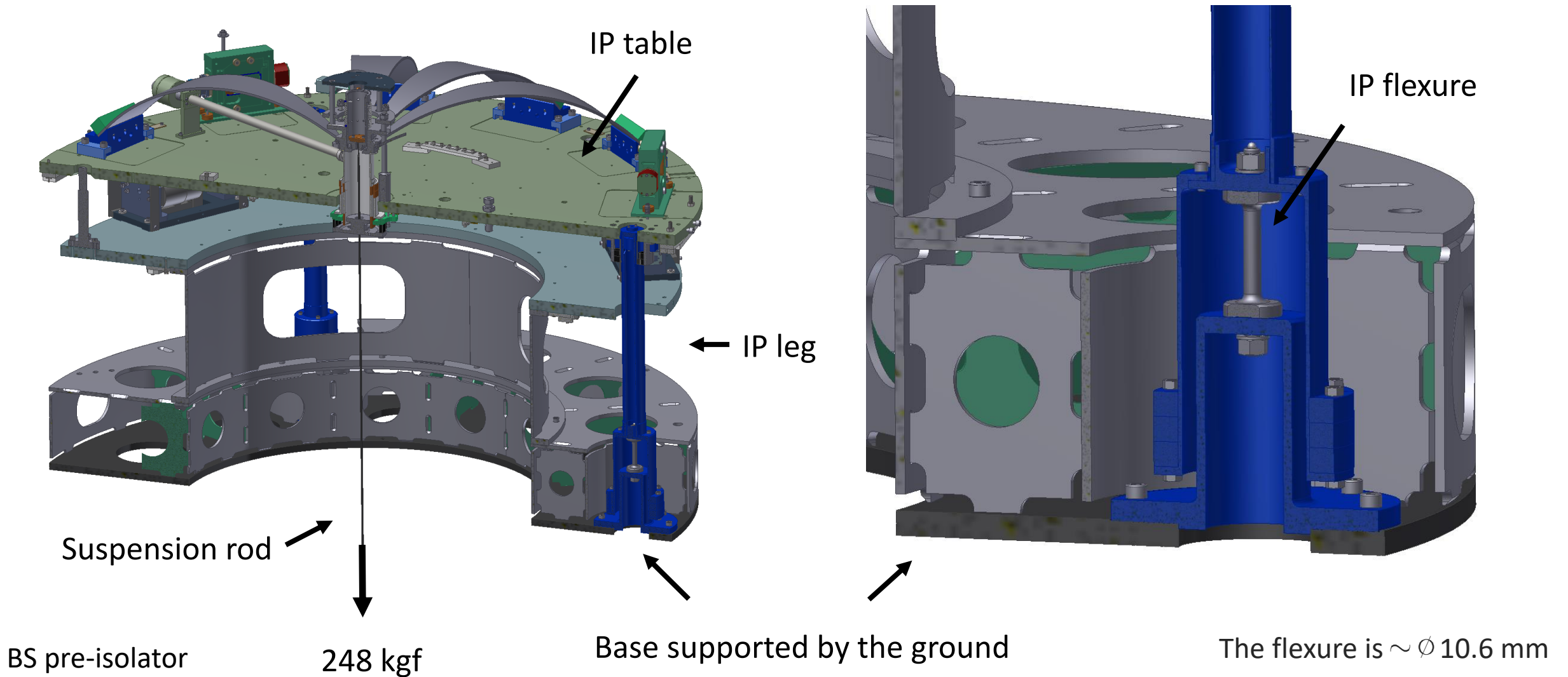
- It filters horizontal vibrations.
- A stiff flexure provides a restoring force for the heavy load.
- When the IP is out of equilibrium the weight of the load produces the anti-spring effect making the system softer.

The weight pulls the load away from equilibrium

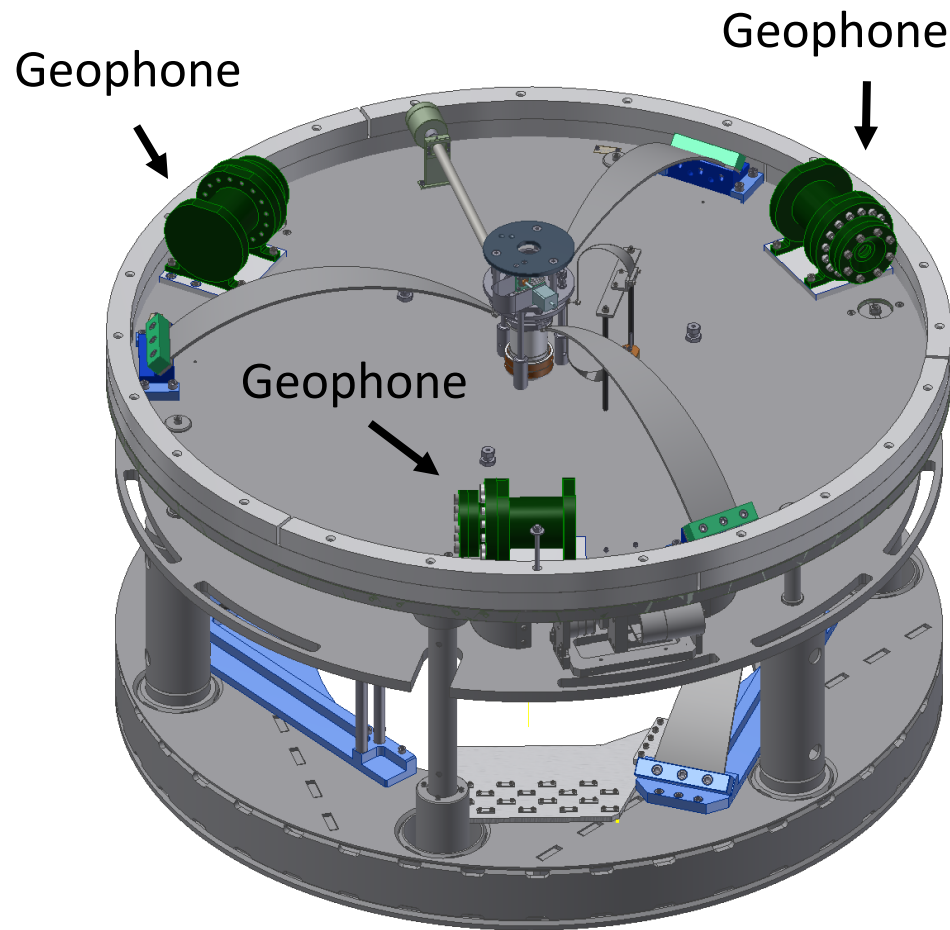


T. Sekiguchi, "A study of low frequency vibration isolation system for large scale gravitational wave detectors," Ph.D. thesis, University of Tokyo, 2016.

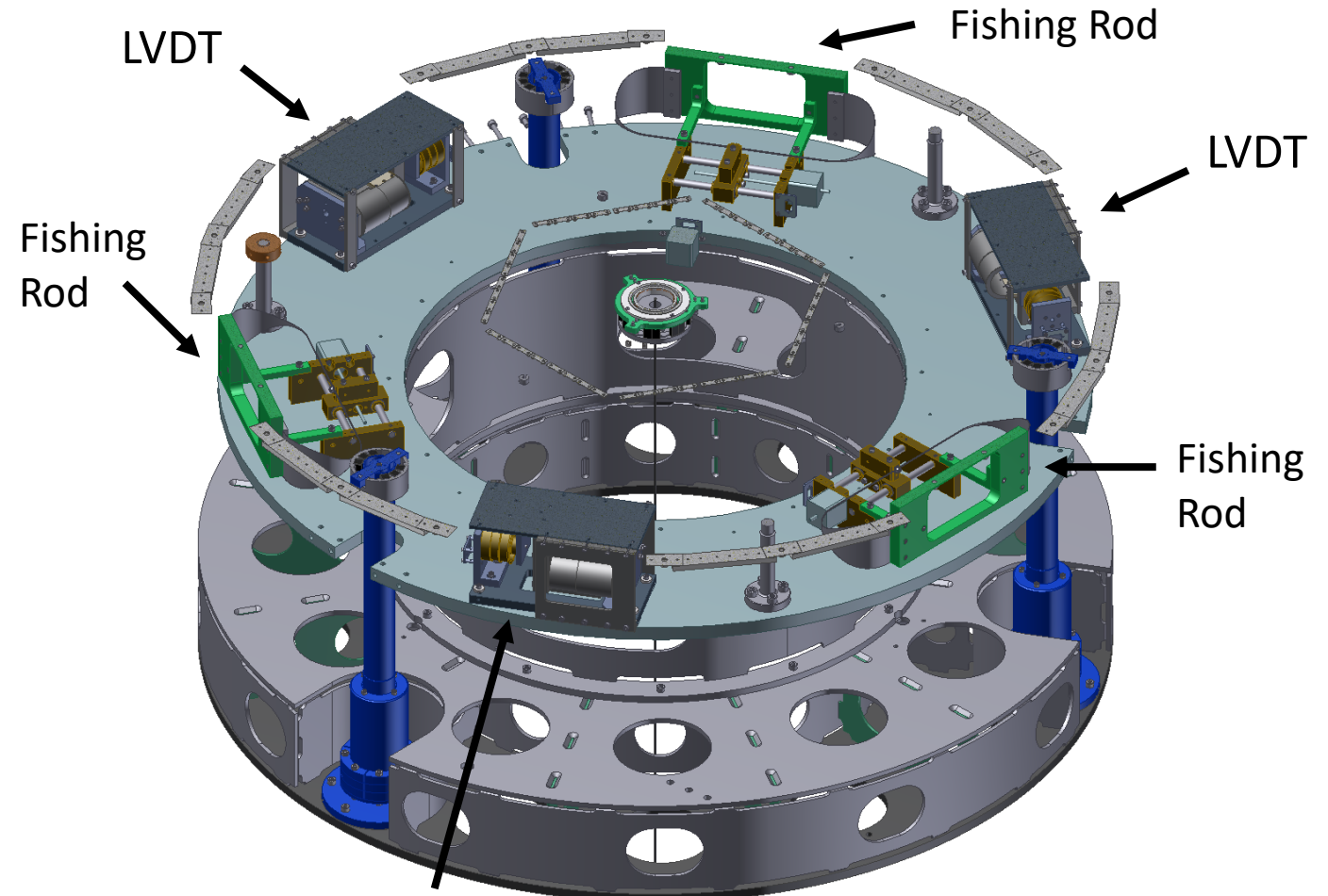
Inverted pendulum components (1)



Inverted pendulum components (2)



SR inverted pendulum

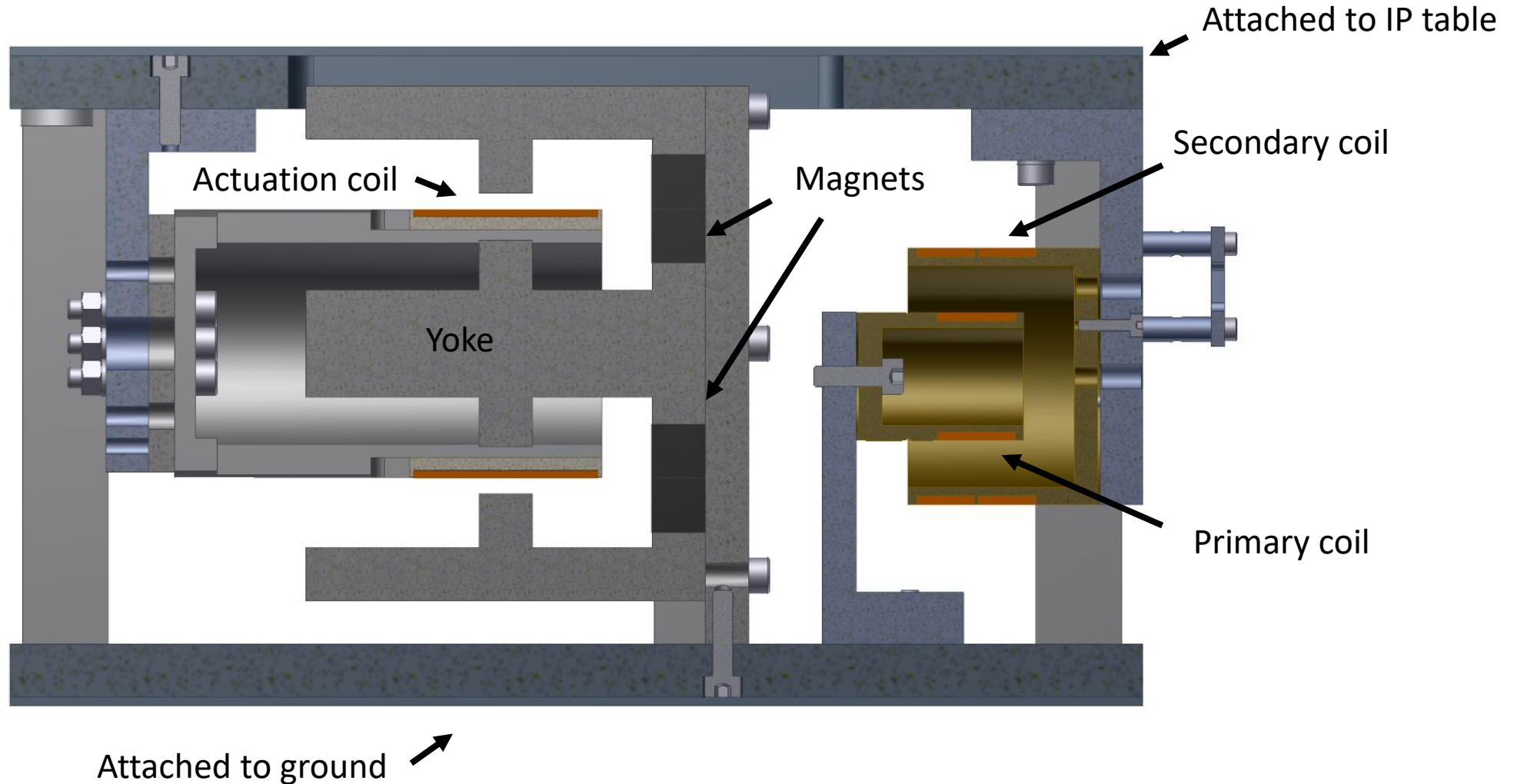


LVDT

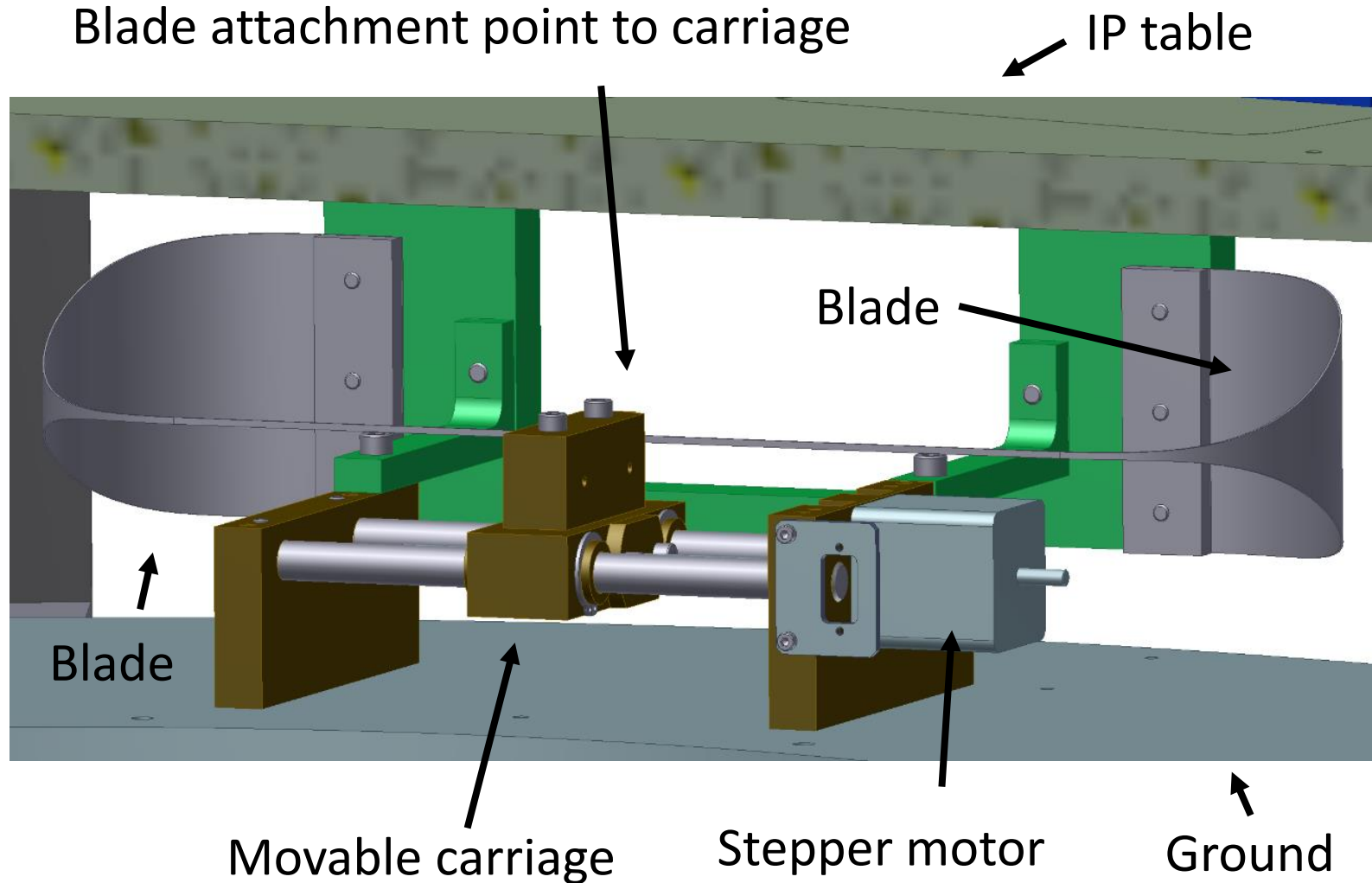
BS inverted pendulum

LVDTs and coil-magnet actuators at the IP

(Linear Variable Displacement Transducer
or any of the other 3 different names)



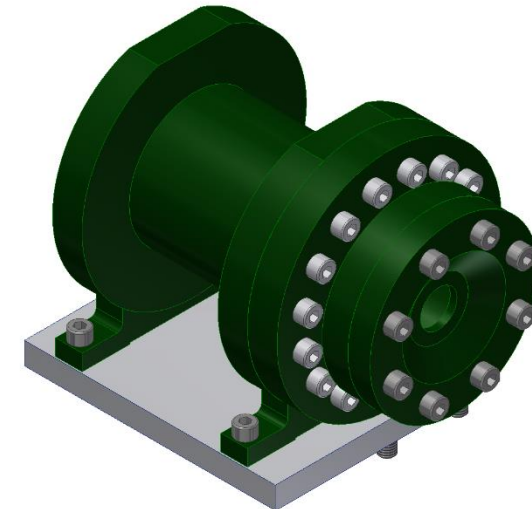
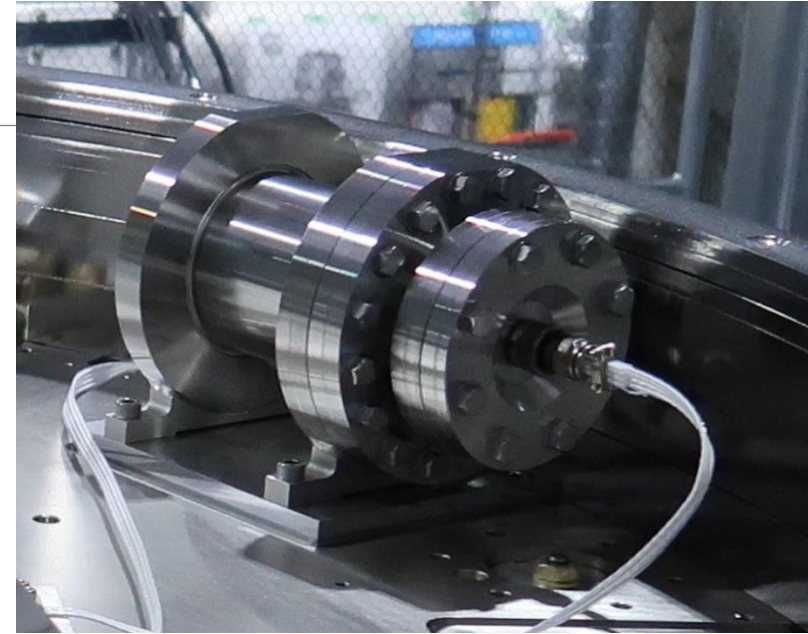
Horizontal fishing rods at the IP



- We can adjust the IP position within several 10s of μm and μrad of the desired position.
- Then we use the coil magnet actuators.

Geophones

- They provide an output proportional to velocity.
- The aim of using the geophones is to damp the micro-seismic peak at around 200 mHz.
- The geophones and the LVDTs are combined into a single sensor using a blending filter:
 - LVDT for position control at low frequencies (aiming at lower than 90 mHz.)
 - Geophones for the micro-seismic peak at 0.2 Hz.
- They are inside a hermetically sealed pod in air.

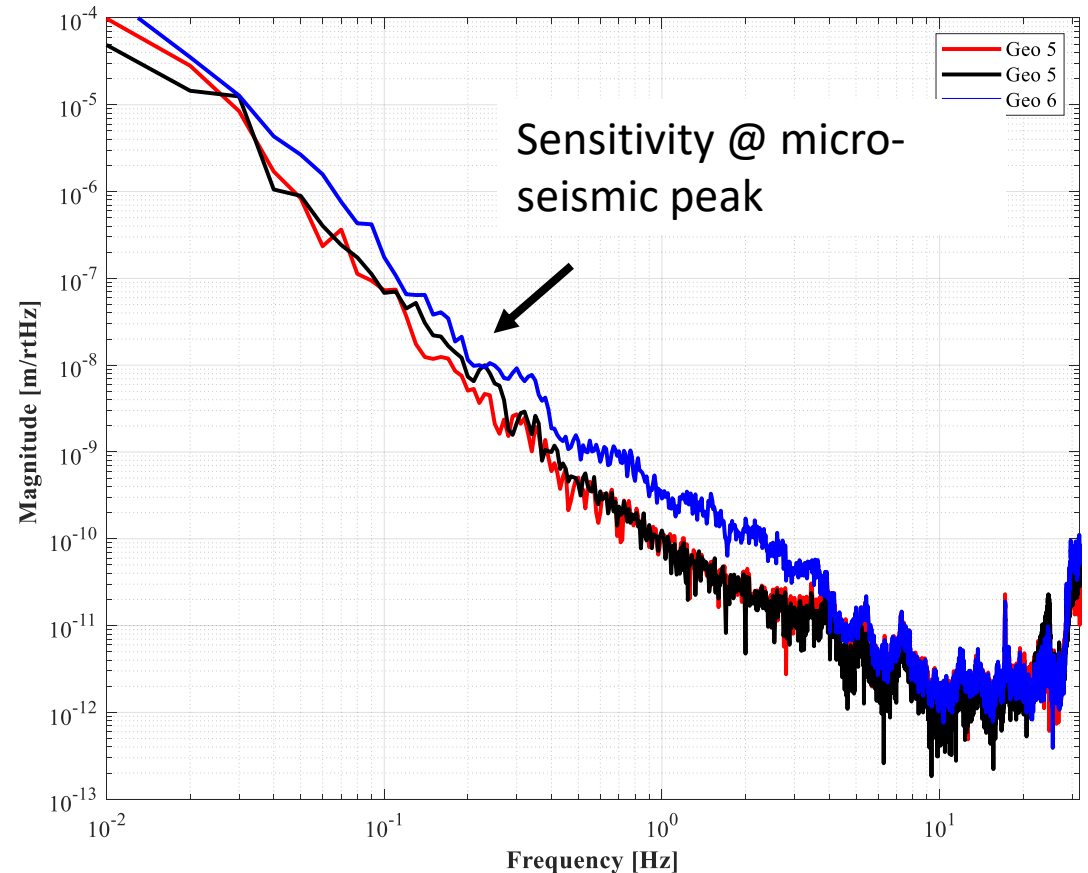


Geophone sensitivity

The noise is measured in sets of three geophones by estimating the correlated and uncorrelated components of their signals.

- Correlated component: ground vibrations at the measurement site.
- Uncorrelated components: the noise of each geophone.

Sleeman et al. **Three channel correlation analysis: a new technique to measure instrumental noise in digitalizer and seismometers.** Bulletin of the Seismological Society of America, vol. 96, issue 1, pp. 258-271



Measured by Yoshinori Fujii

Geophones calibration

- Geophone respond to ground velocity:

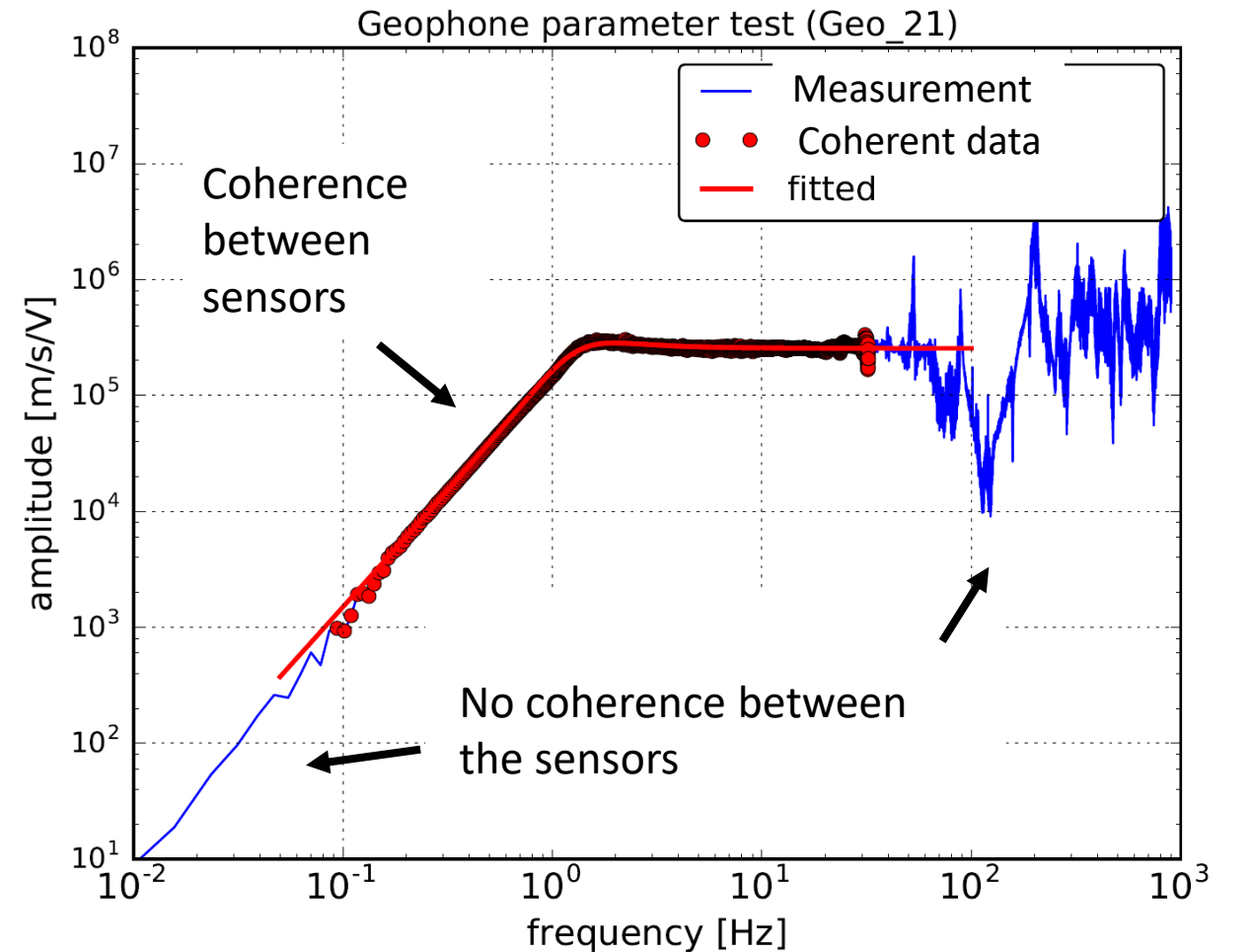
$$H_{GEO}(\omega) = \frac{G_e \omega^2}{\omega_0^2 + 2i\eta\omega\omega_0 - \omega^2}$$

G_e : constant [V/m/s].

η : intrinsic damping ratio.

ω_0 : resonant frequency [rad/s].

- They are calibrated using a reference device.

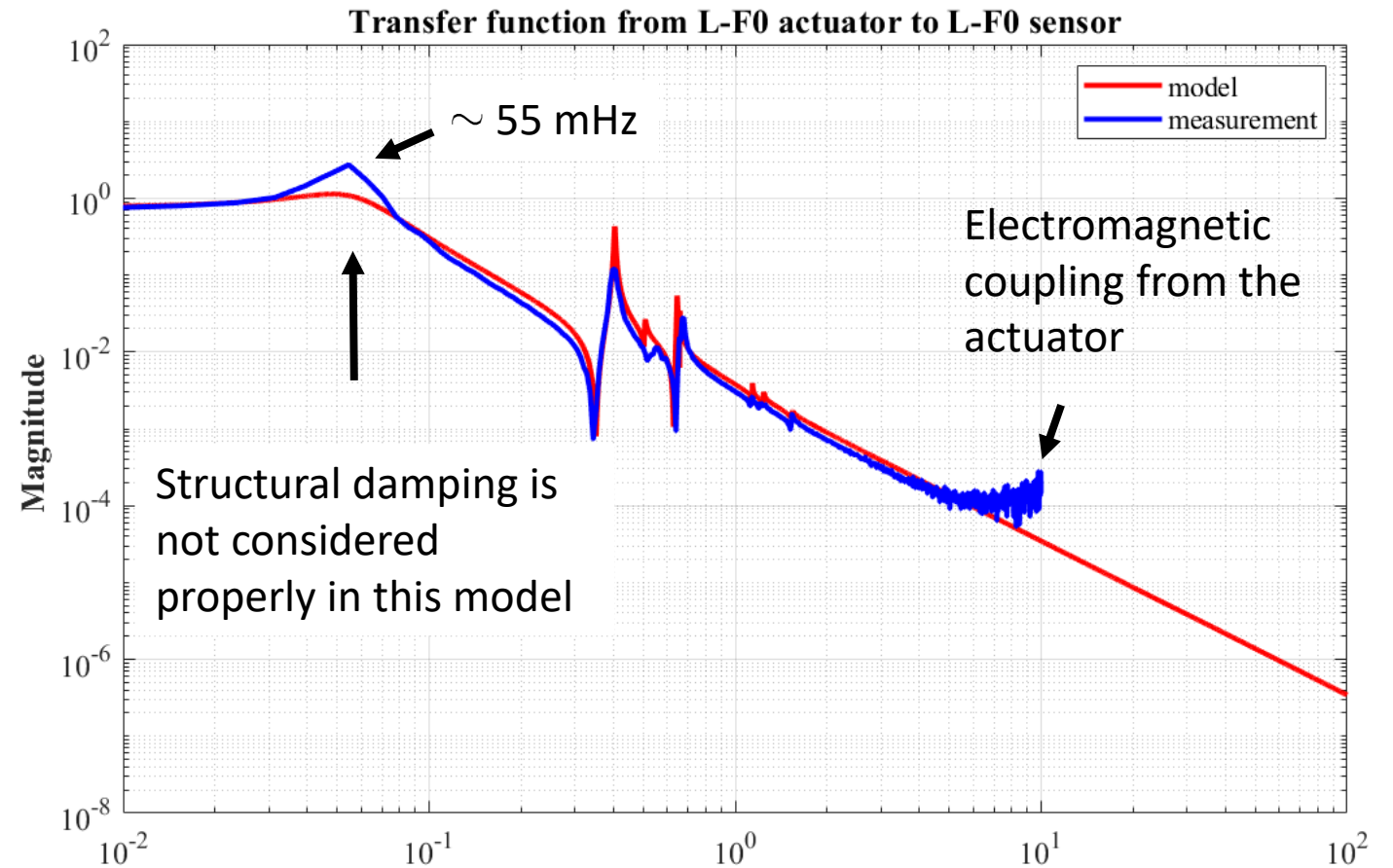


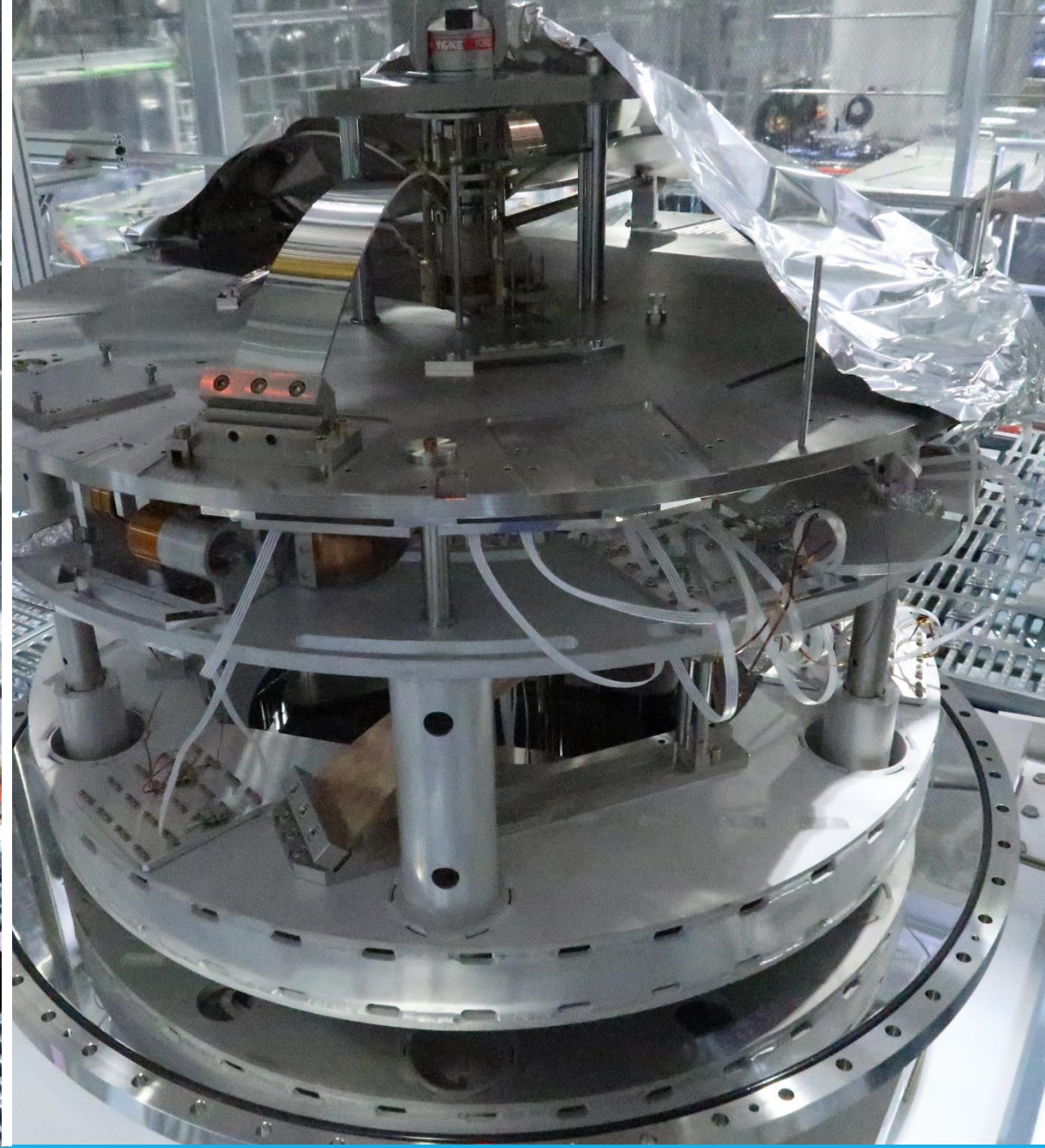
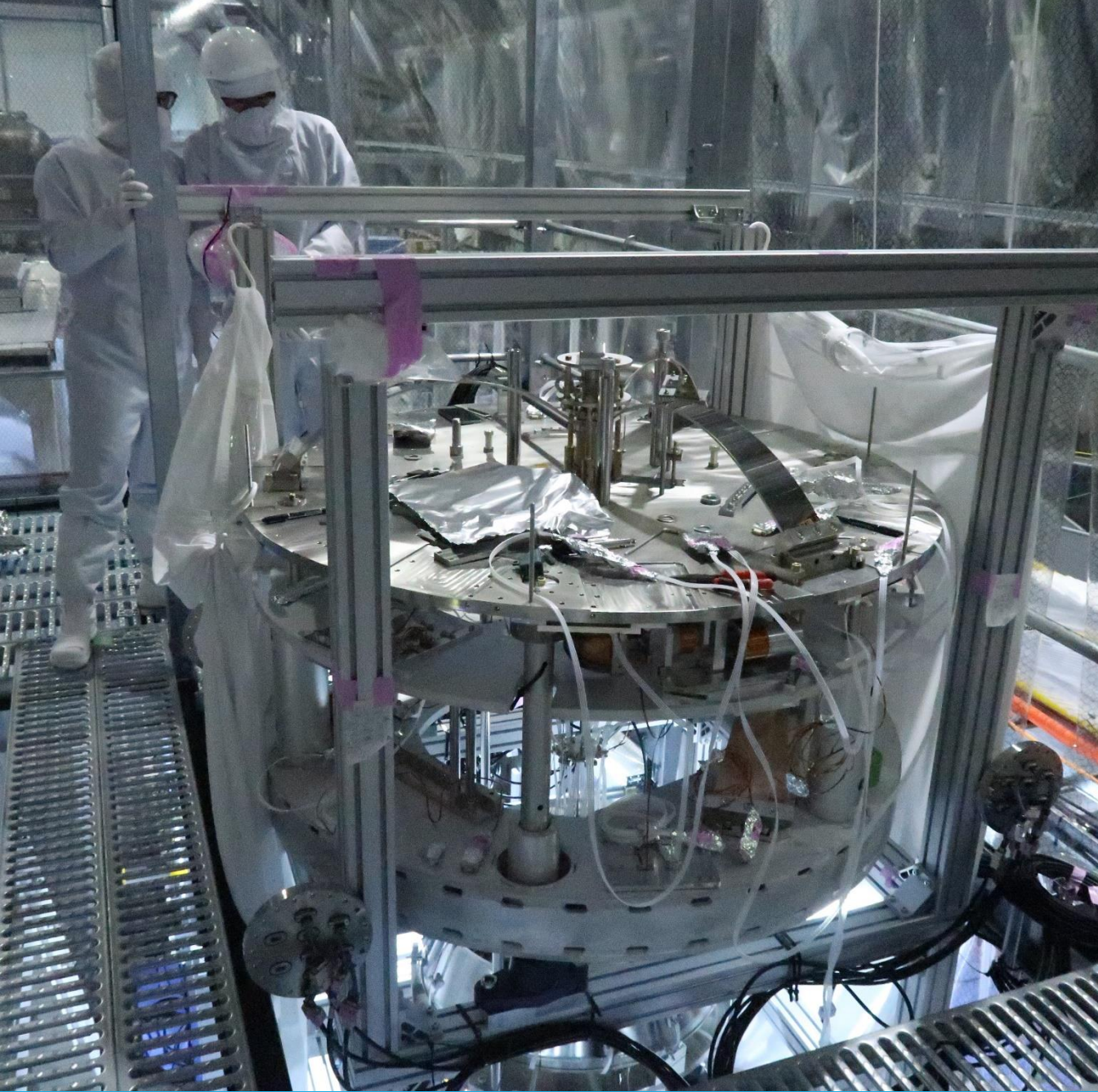
Measured by Yoshinori Fujii

Inverted pendulum properties

Resonant frequencies for the SR2 IP:

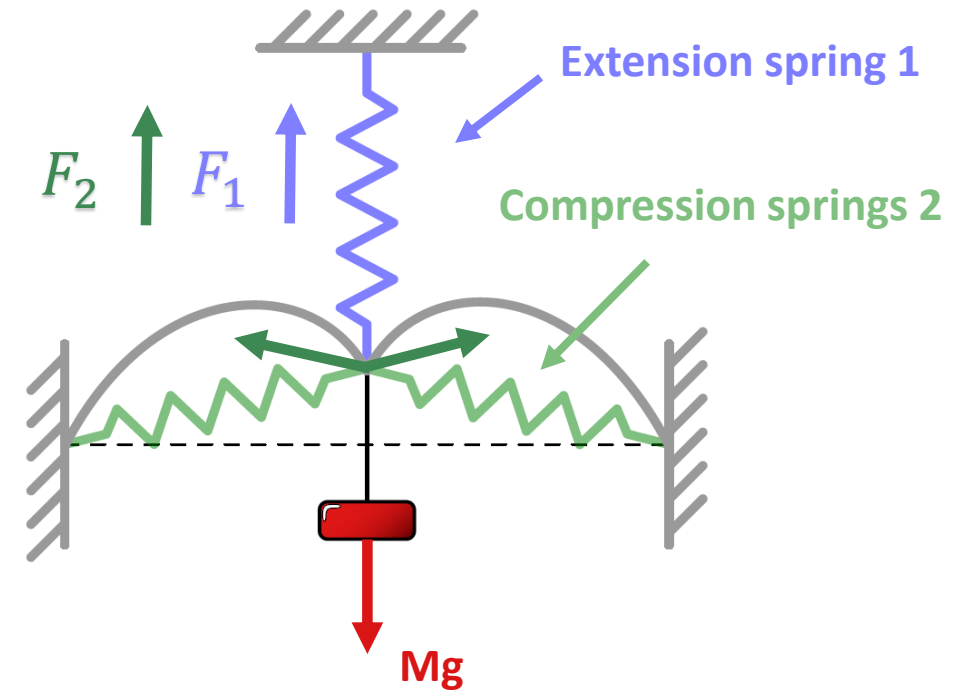
- Longitudinal: ~ 55 mHz.
- Transverse: ~ 55 mHz.
- Yaw: ~ 300 mHz.





Geometric anti-spring

- It filters vertical vibrations.
- The extension spring is very stiff so it can support a heavy load.
- The compression springs push the load away from the equilibrium position as the load moves: the system becomes softer.

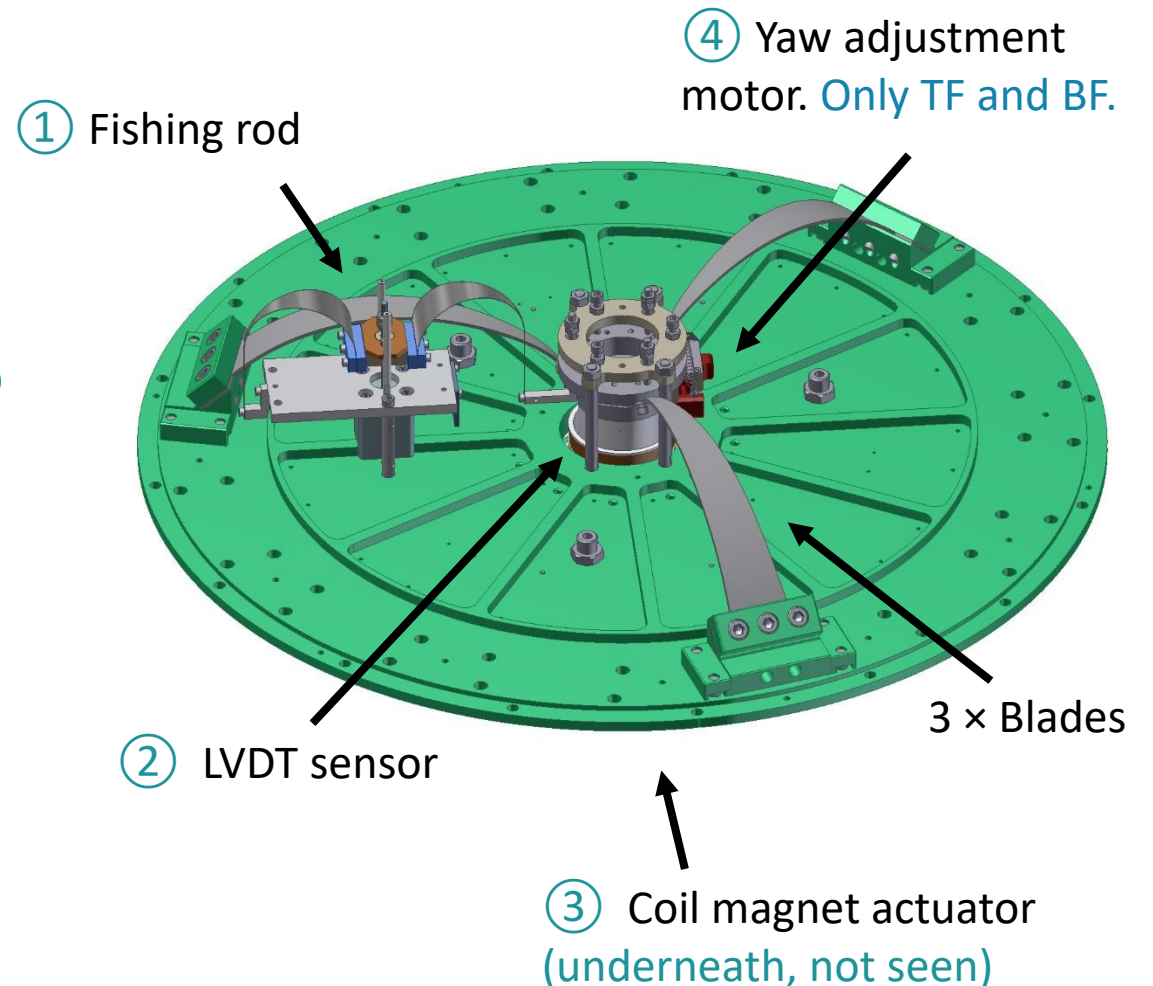


Original drawing by Alexander Wanner

GAS filters in the Type B suspension

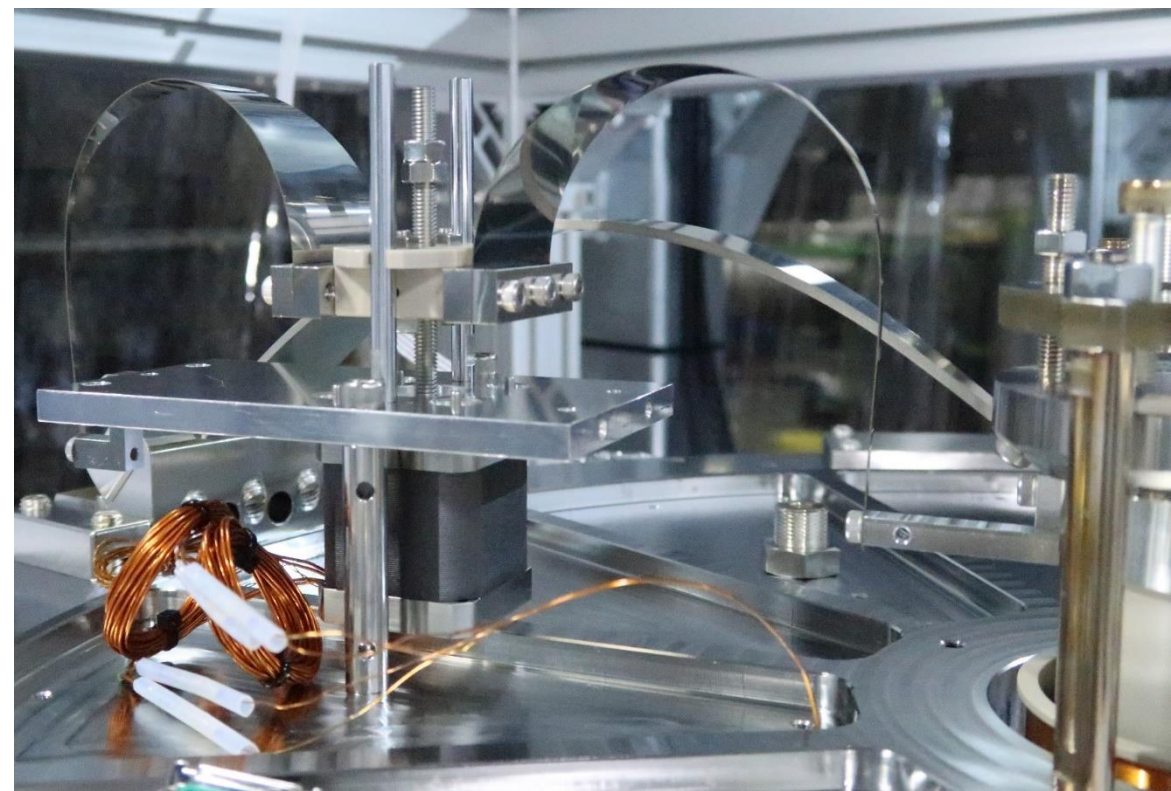
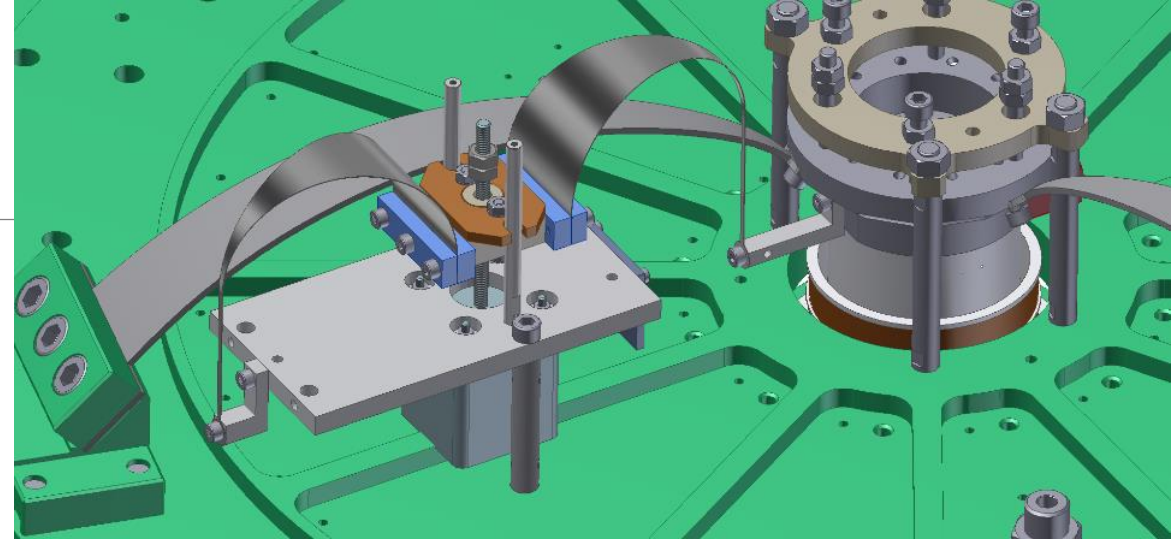
Similarities and differences:

- All of them have fishing rod actuators. ①
- All of them have LVDT displacement sensors. ②
- All of them have coil-magnet actuators. ③
- Yaw adjustment motor: **Top Filter and Bottom filter.** ④
- Magnetic damper ring: **only Standard Filter.**
- The Intermediate Recoil Mass (IRM) hangs directly from the **Bottom Filter** base plate. (It will be shown later.)
- The **Bottom Filter** has tilt mechanism to finely adjust the position of the IRM. (Not shown.)

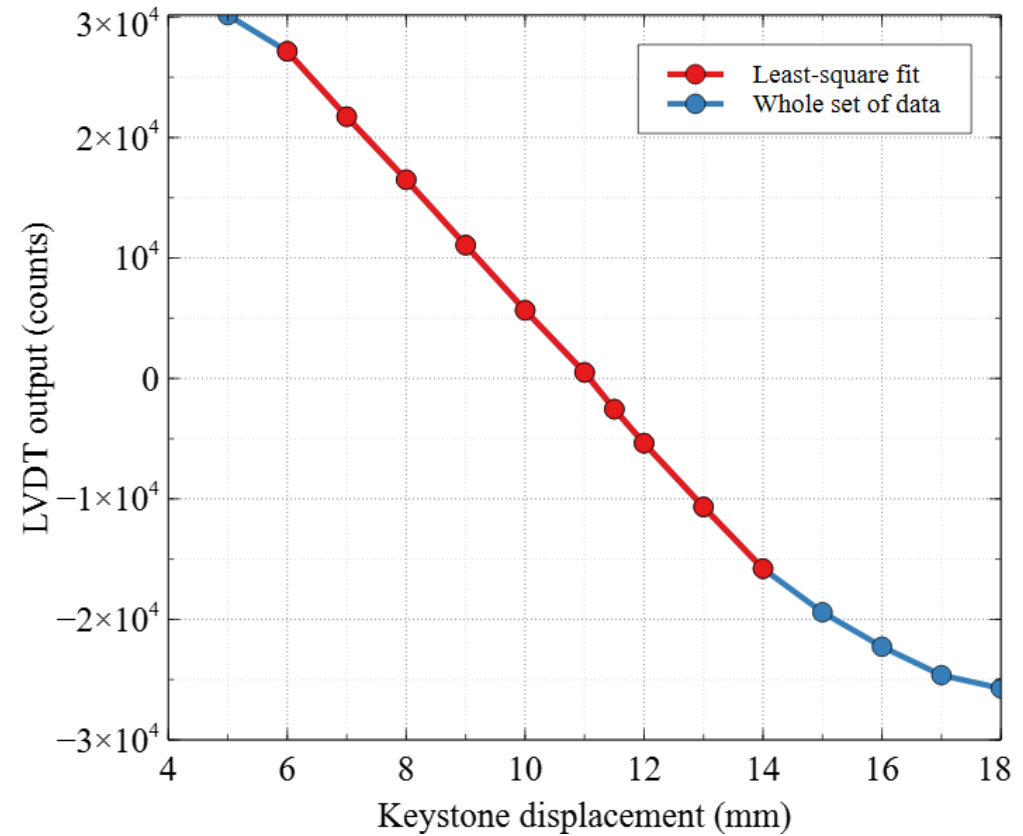
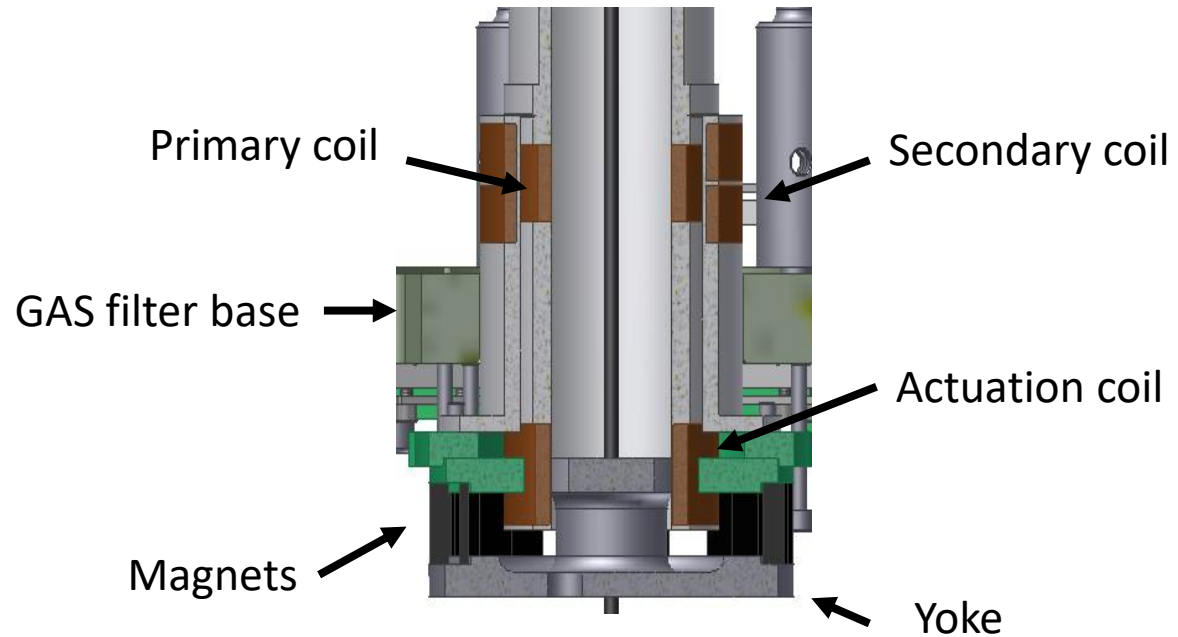


Fishing rods

- Its aim to finely adjust the position of the load:
 - We need to set the optic at the correct height.
 - The keystone has to be at the right height.
- We usually have to move it by **tens of microns at the time** and then use the coil magnet actuator to take it to the desired position.
- **This is not used in the control loop.**



LVDT calibration



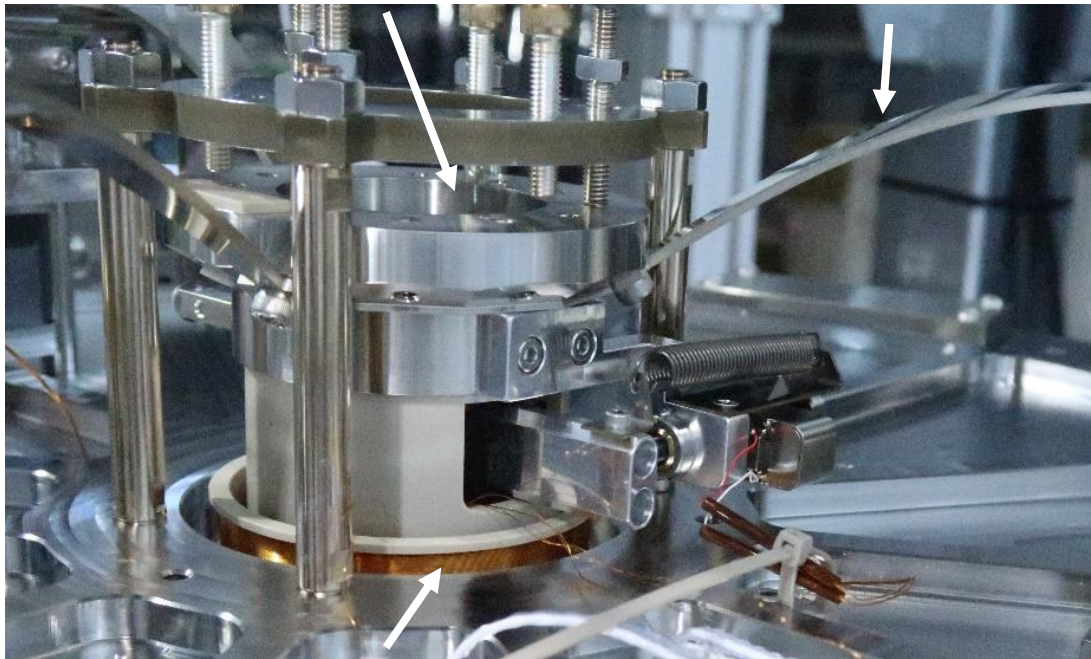
- Example: F0 LVDT in SRM
- Calibration factor example: $-0.185 \mu\text{m}/\text{count}$.
- Linear range: 8 mm.

LVDT and coil-magnet actuators

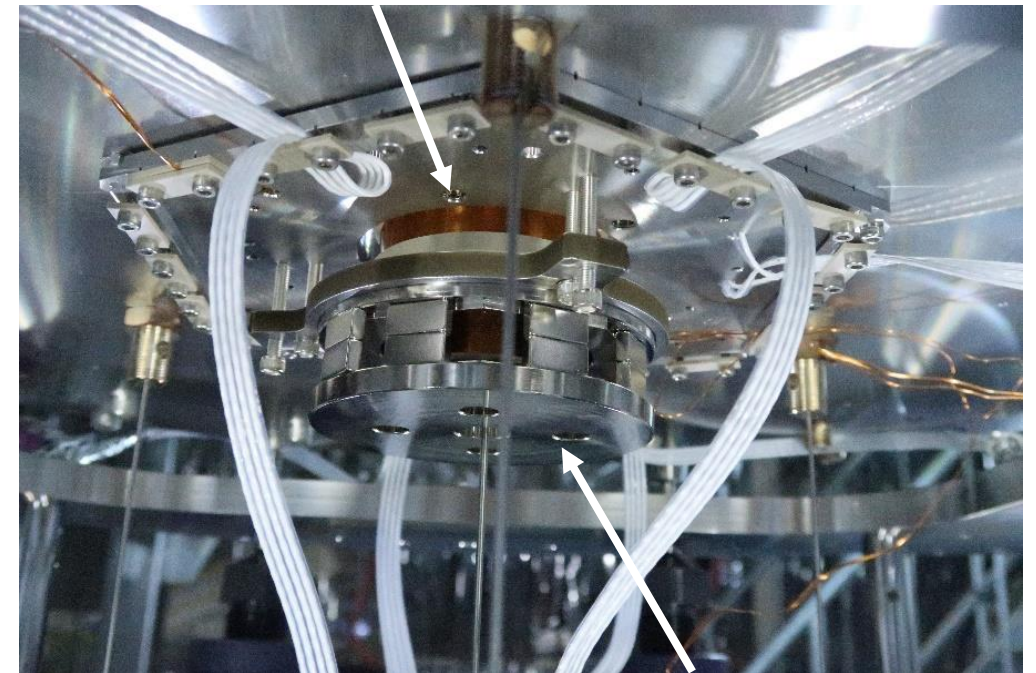
Keystone

Blade

Actuation coil



LVDT secondary coil

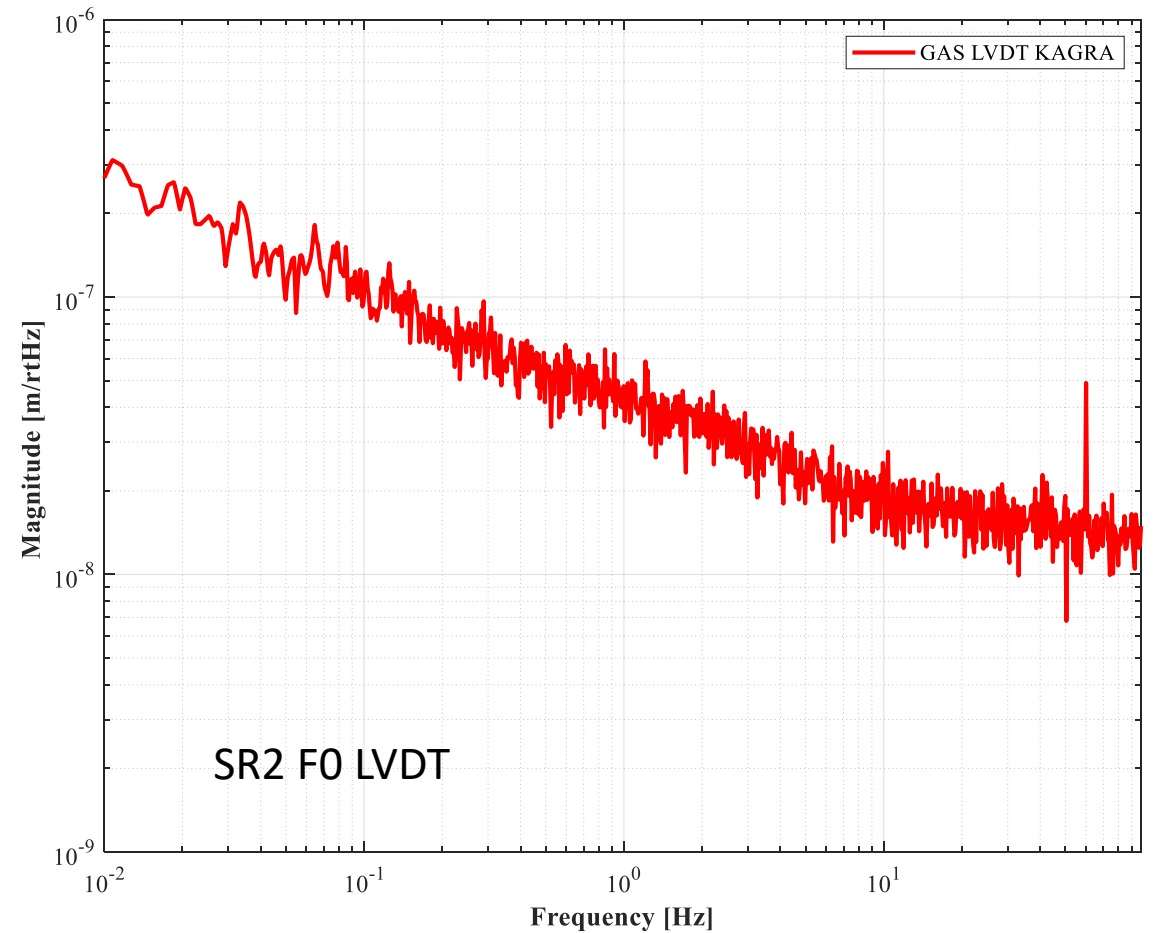


Yoke

Suspension rod at the centre of coils

LVDT sensitivity

- It was measured by locking the LVDT.
- At 1 Hz: $0.04 \mu\text{m}/\sqrt{\text{Hz}}$.
- At 10 Hz: $0.02 \mu\text{m}/\sqrt{\text{Hz}}$.
- Integrated RMS: typical values from 0.1 to $0.5 \mu\text{m}$.

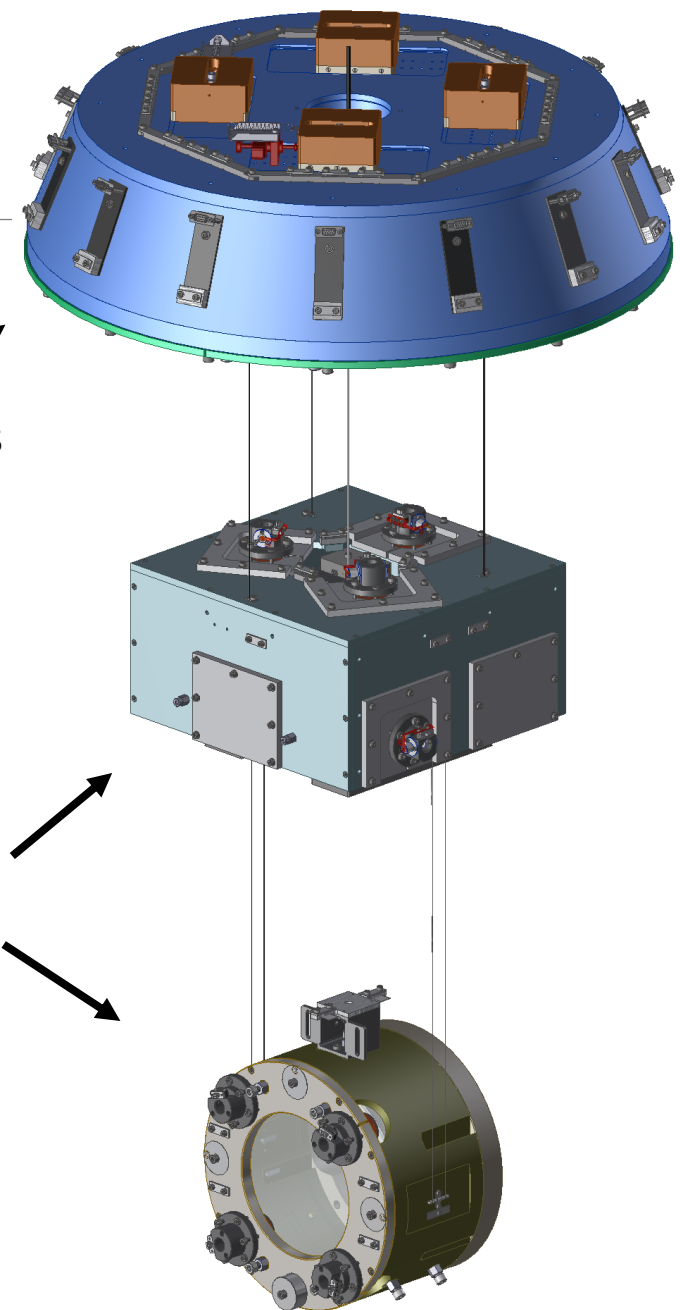


The payload (1)

- Optic:
 - it has magnets for applying forces with coils.
 - It has primary and secondary wire breakers.
- Recoil Mass: it holds coil for applying forces onto the optic.
- Intermediate Mass (IM)
 - It holds the optic and the Recoil Mass with wires.
 - It serves as a marionette for roll and pitch.
 - Yaw is adjusted with either the Bottom Filter or Top Filter.
 - It has OSEMS to actively damp the resonant modes of the payload itself.
- Intermediate Recoil Mass:
 - Holds the OSEMS.
 - Hangs from the BF with three suspension rods.
- Oplev on the ground for measuring pitch, yaw and longitudinal.

The payload hangs from the BF

Payload

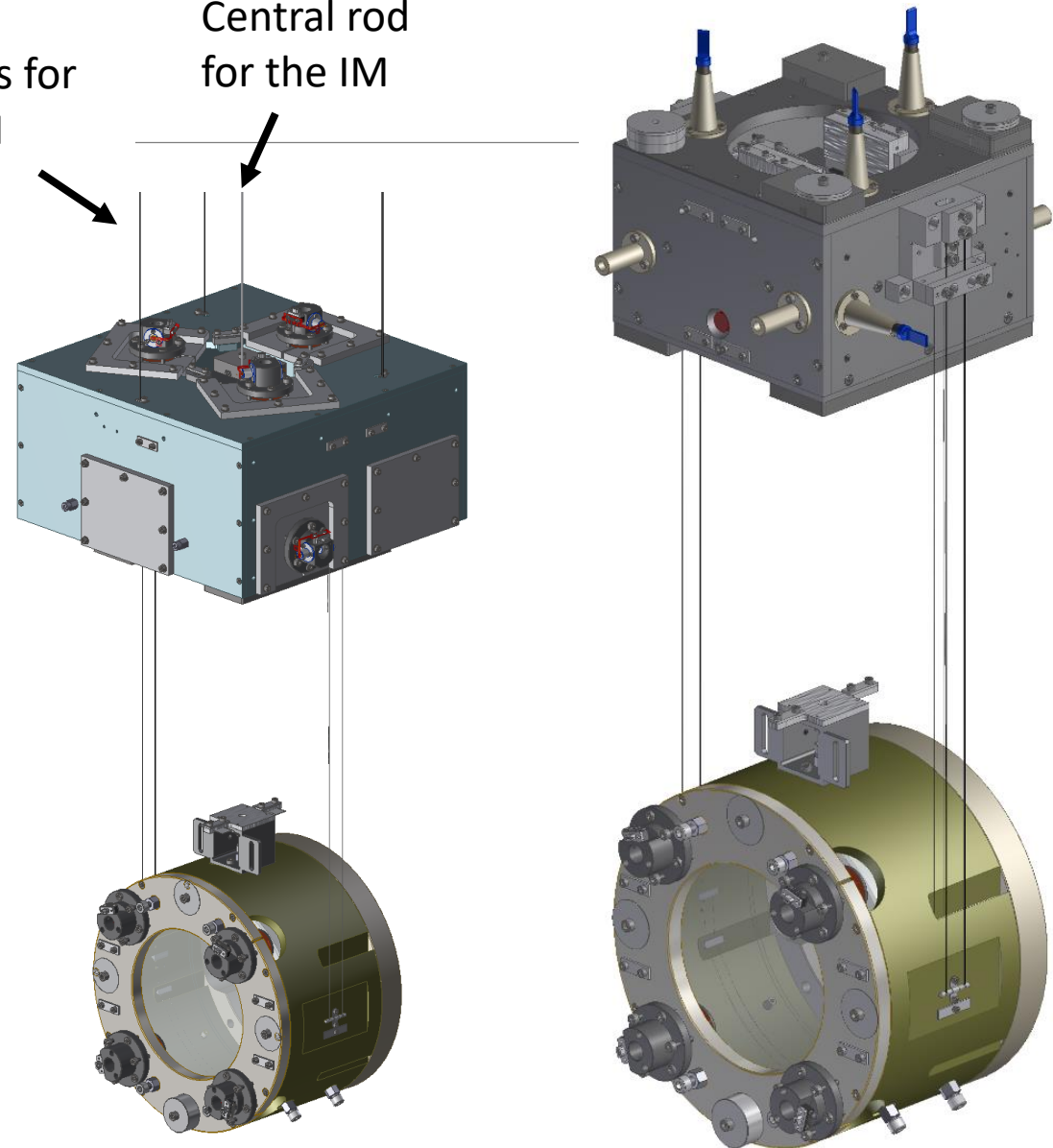


The payload (2)

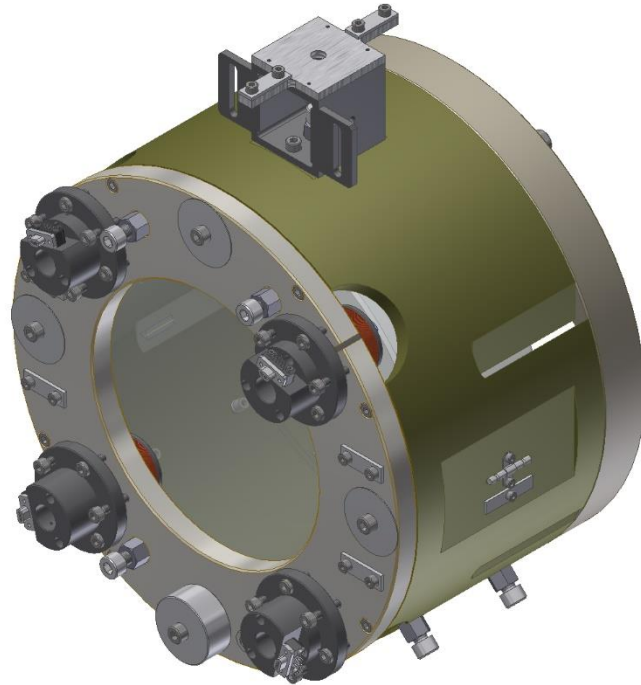
- IRM: 3 × 2 mm maraging rod.
- IM: 1 × 2 mm maraging rod (neck).
- Optic: 2 × loops of piano wire 200 μm thick.
- RM: 2 × loops of tungsten wire 650 μm tick.
- IRM: aluminium, 8.9 kg.
- IM: aluminium and stainless, 26.2 kg.
- Optic: fused silica, 10.2 kg.
- RM: titanium, 12.0 kg.

3 × Rods for
the IRM

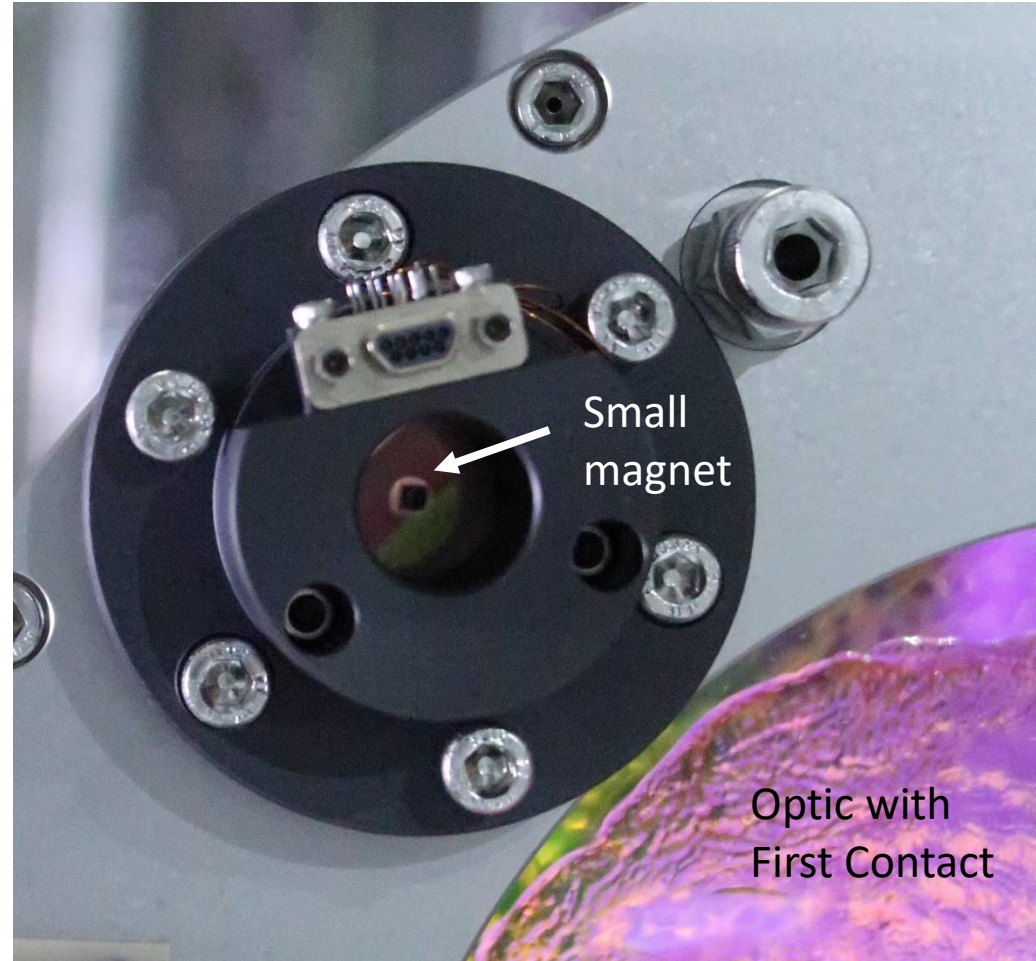
Central rod
for the IM



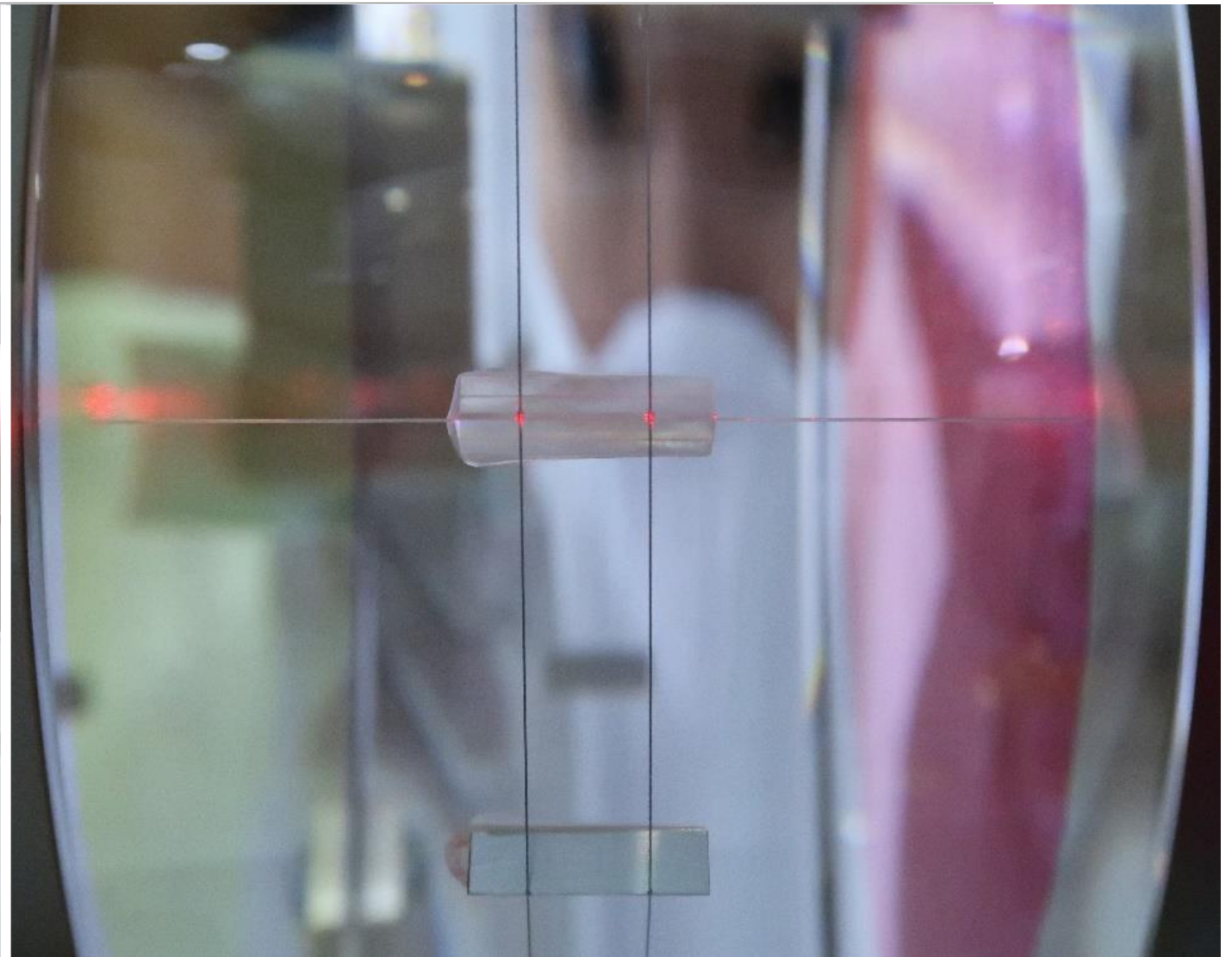
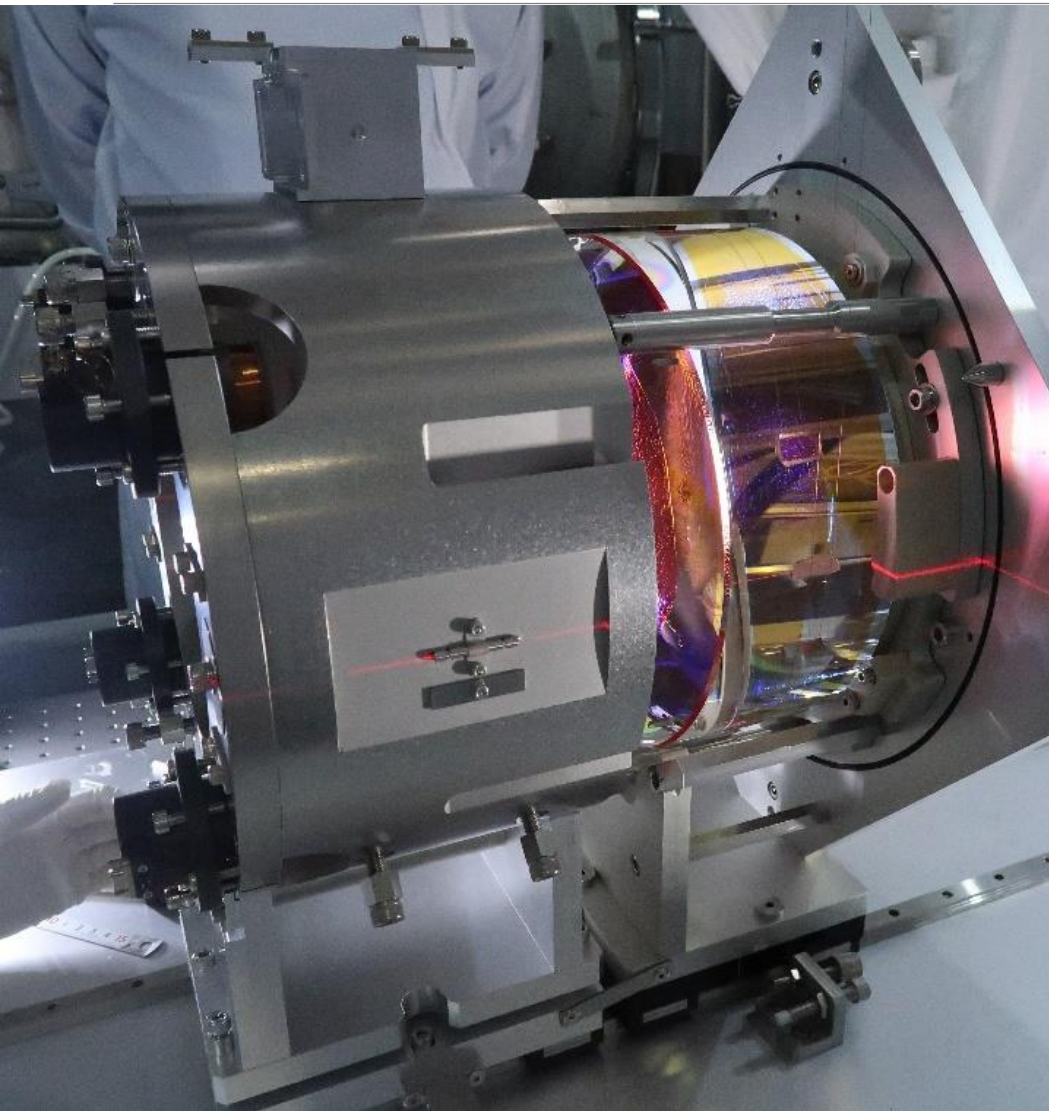
The Optic and the Recoil Mass (1)



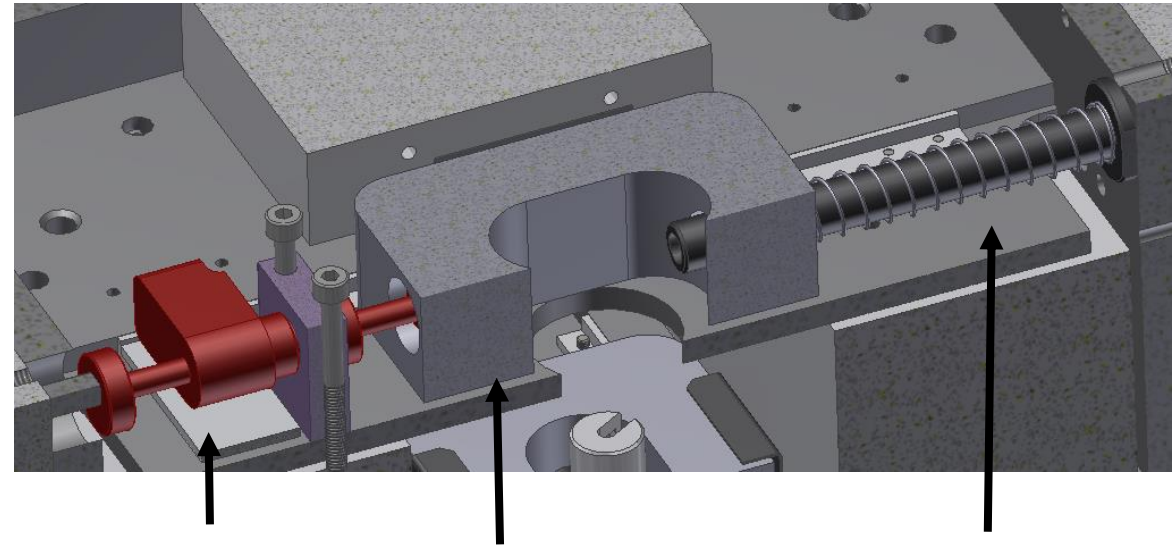
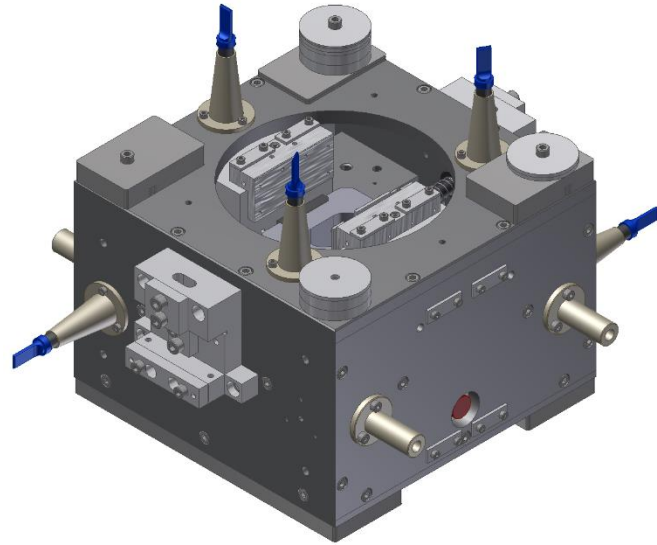
The centres of mass of the optic and RM coincide, nominally.



The Optic and the Recoil Mass (2)



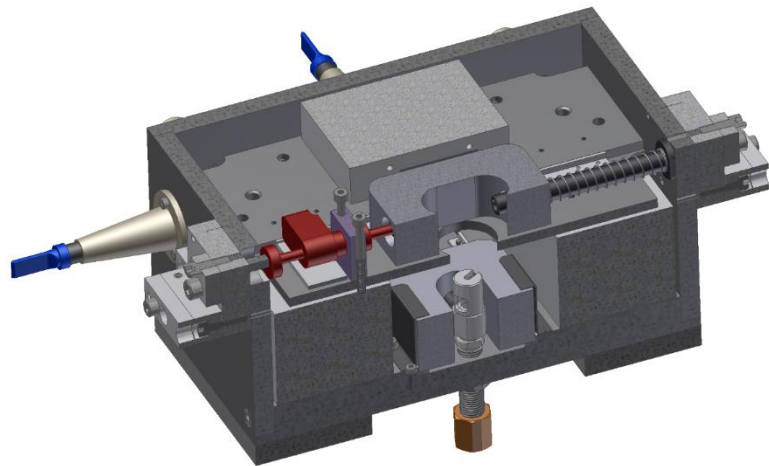
The Intermediate Mass marionette (1)



Pico-motor actuator

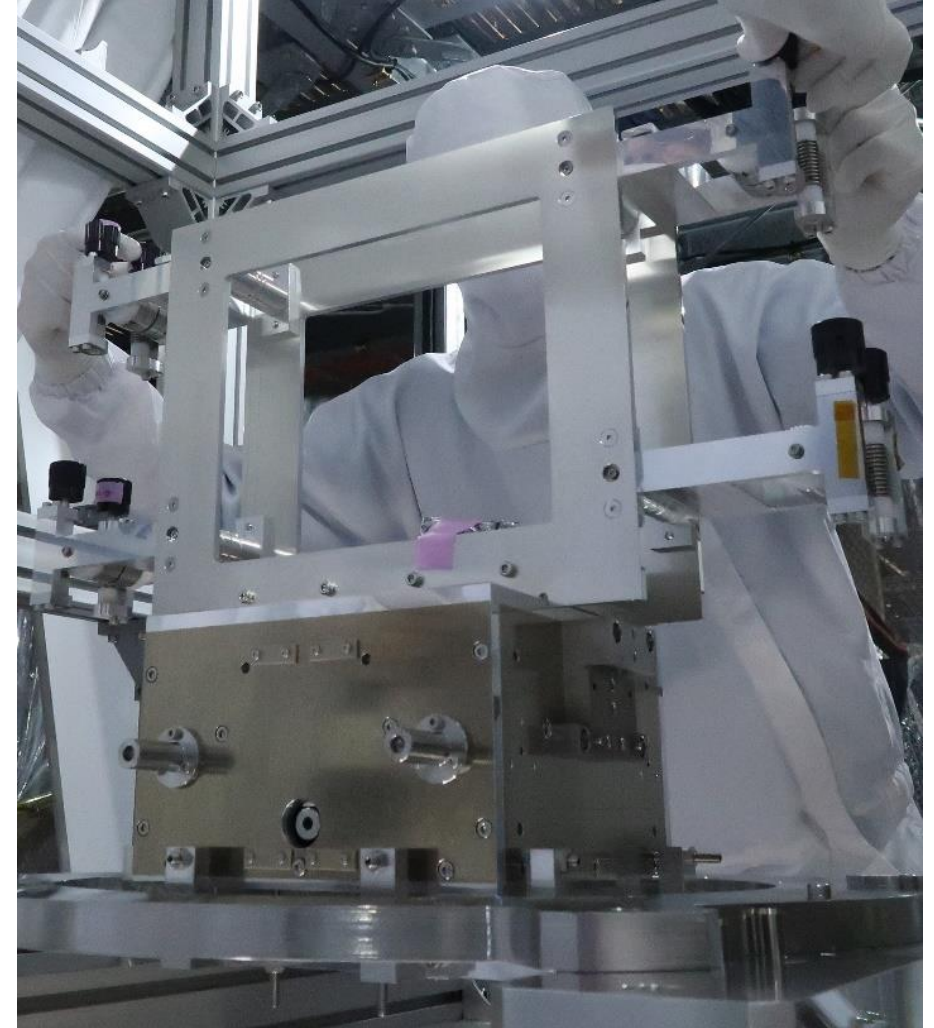
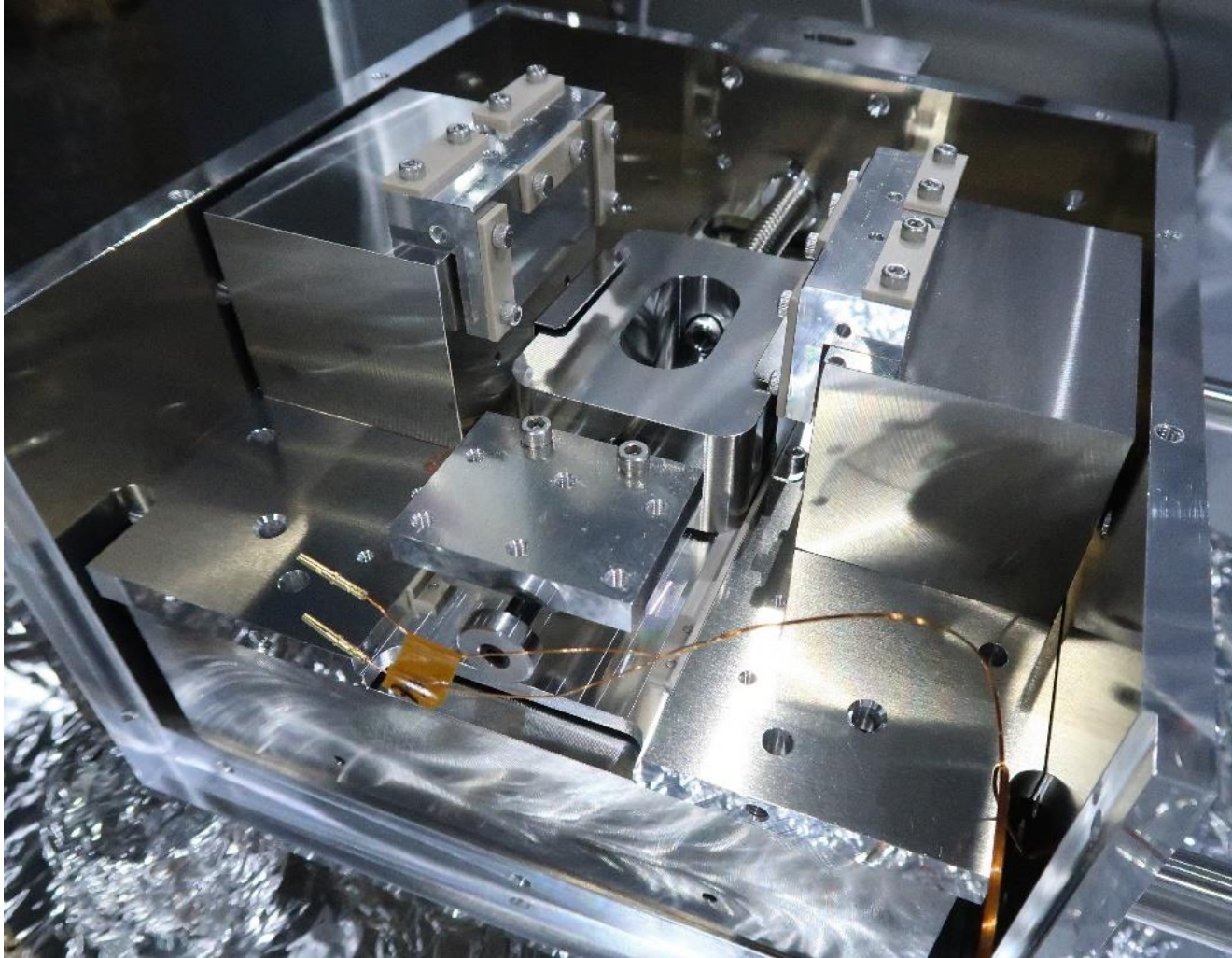
Movable mass

Spring

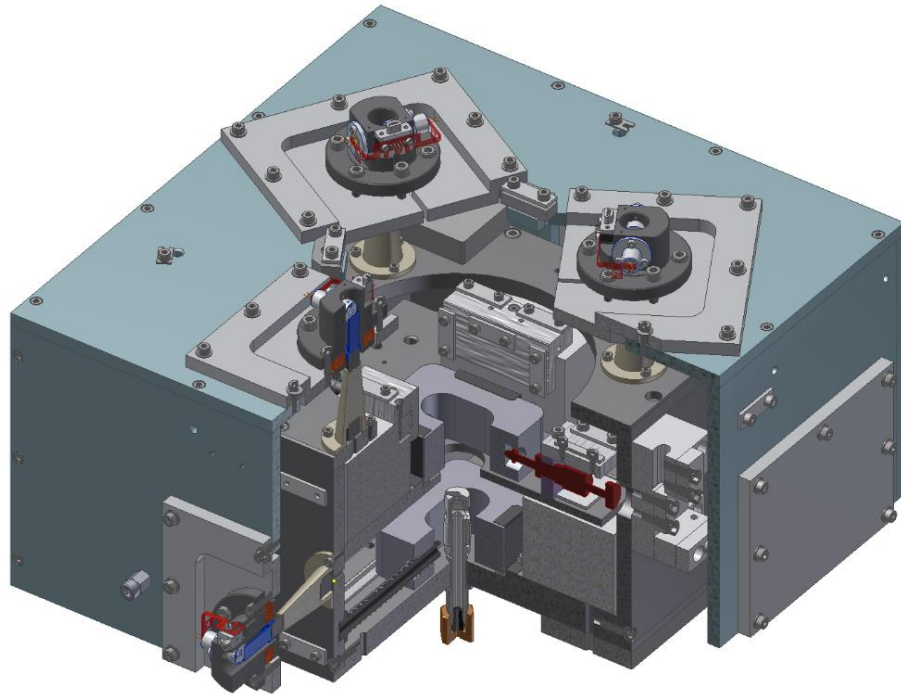


- We can tilt the marionette in roll and pitch by changing the position of its centre of mass with sliding masses within.
- We tend to adjust within a few μrad from desired position and then use coil magnet actuation.

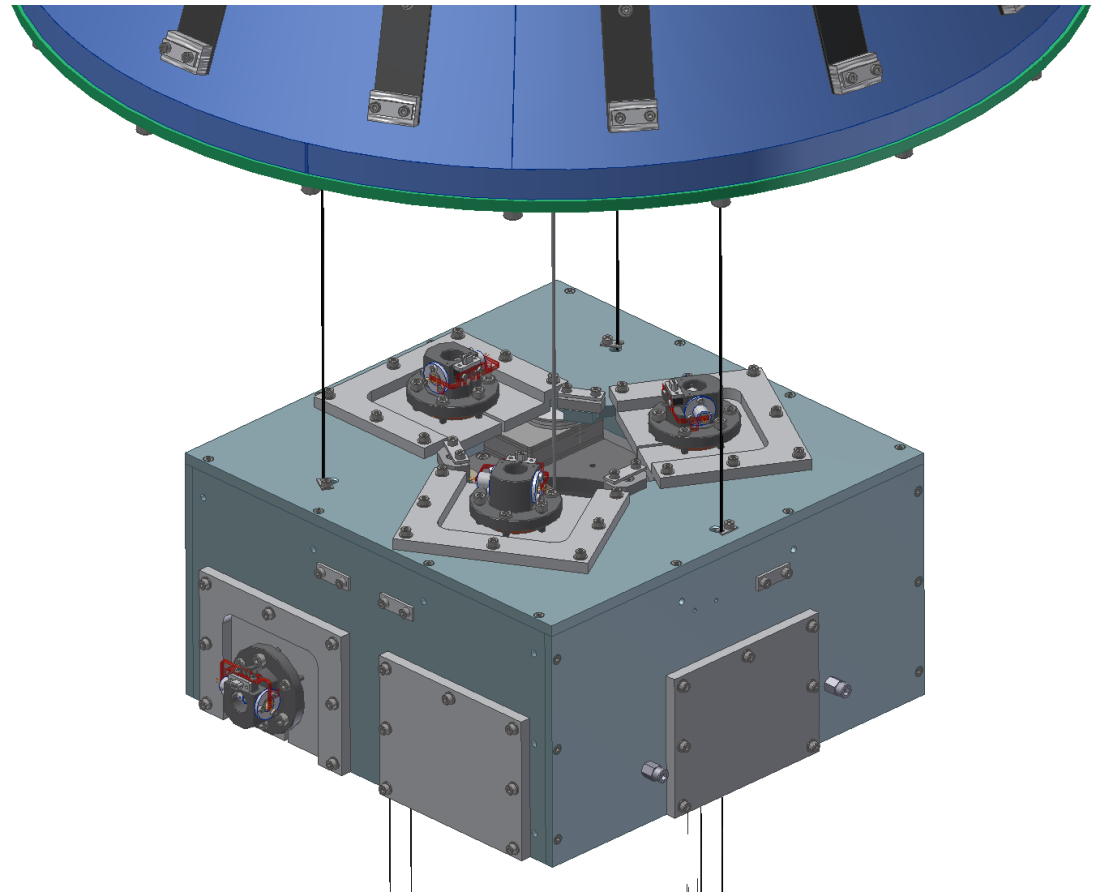
The Intermediate Mass marionette (2)



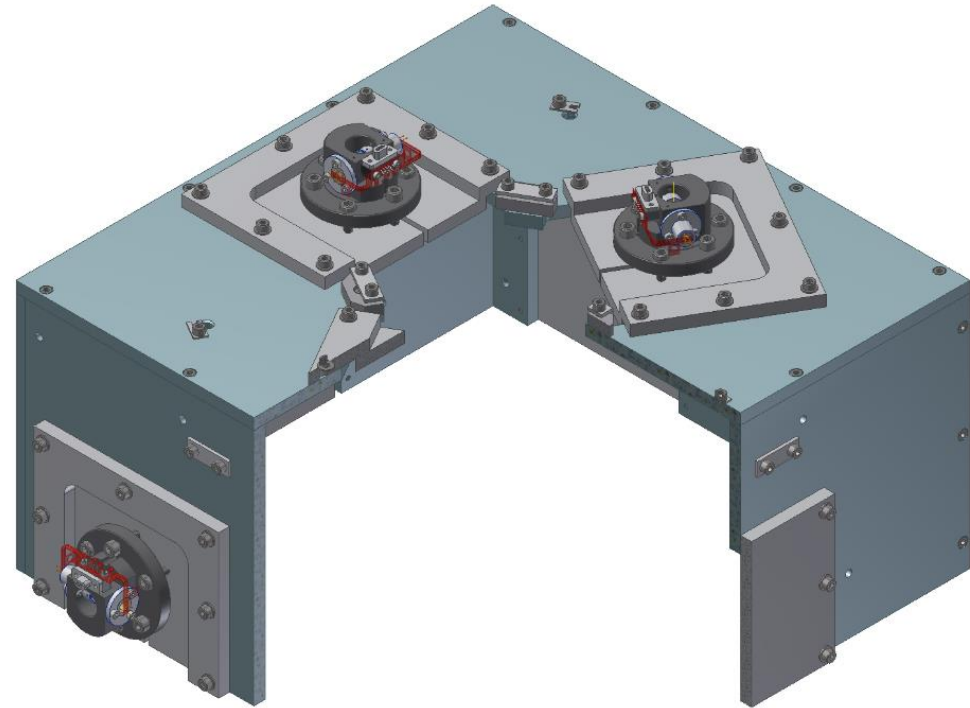
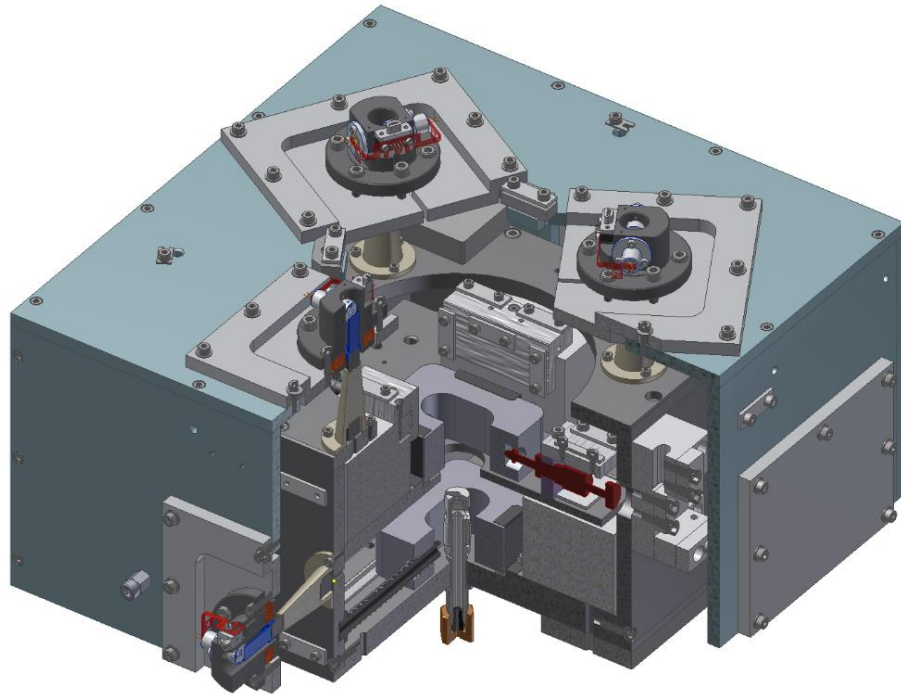
Intermediate Recoil Mass



- The RM is a box opened at the bottom.
- It holds the OSEMs.
- It hangs from the BF

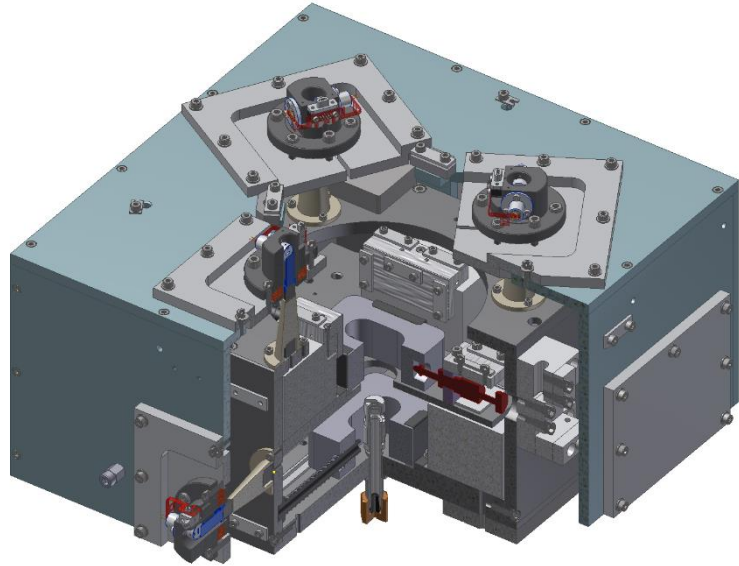


Intermediate Recoil Mass

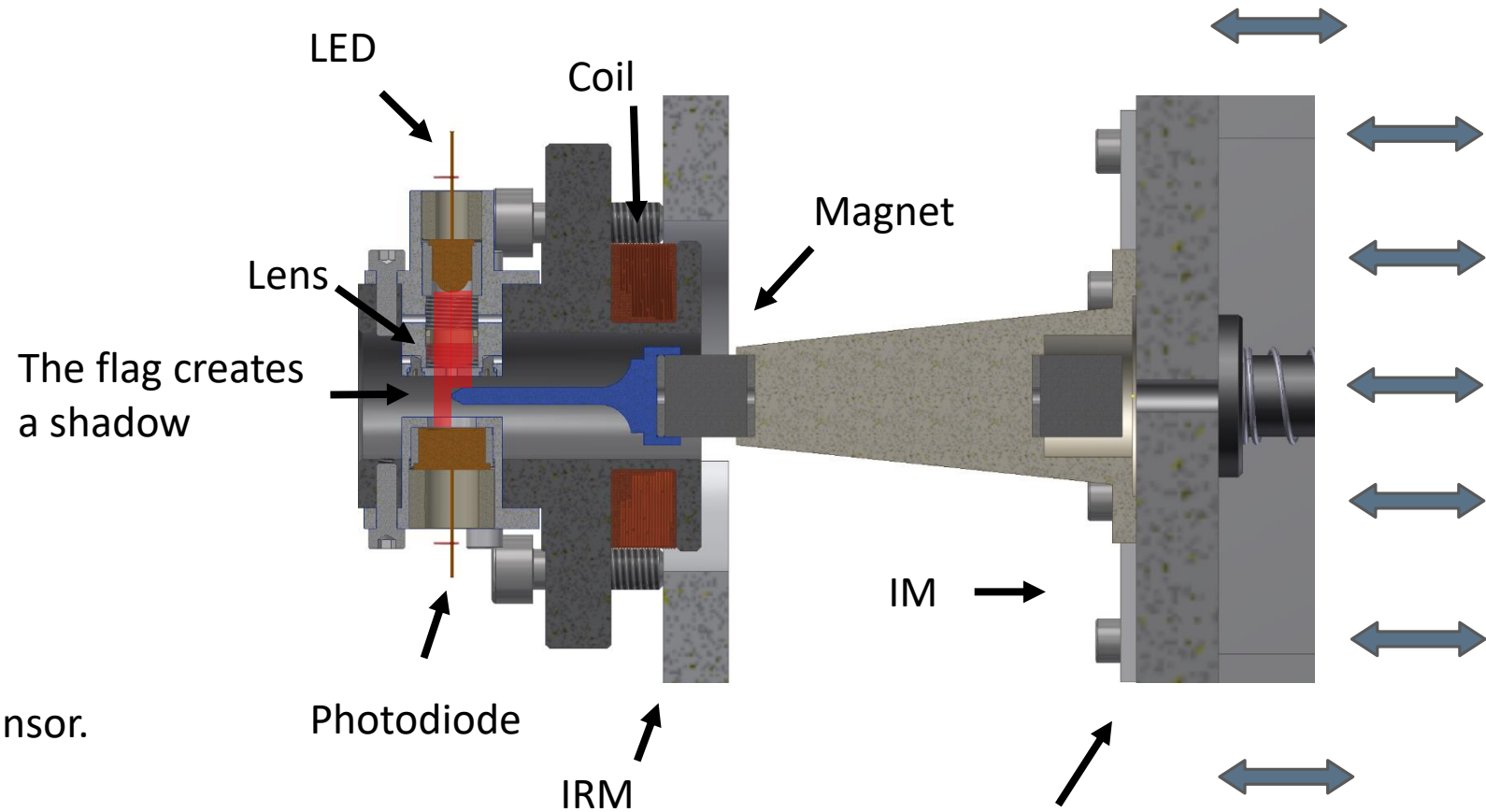


- The RM is a box opened at the bottom.
- It holds the OSEMs.
- It hangs from the BF

OSEM: Optical Sensor and Electromagnetic Actuator



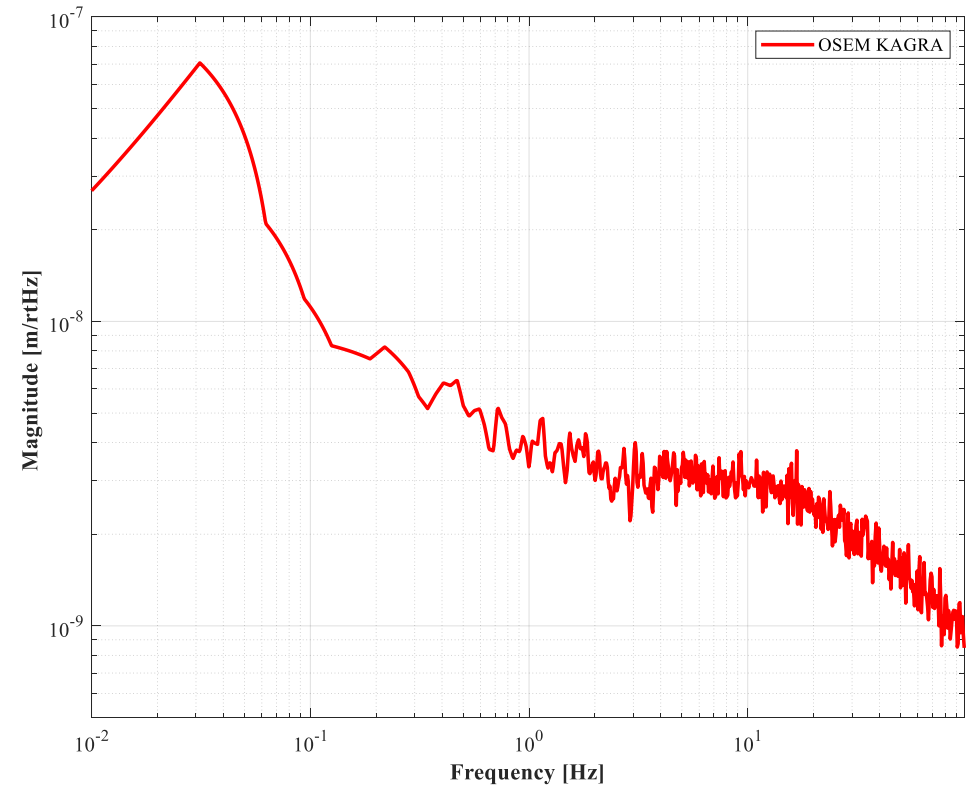
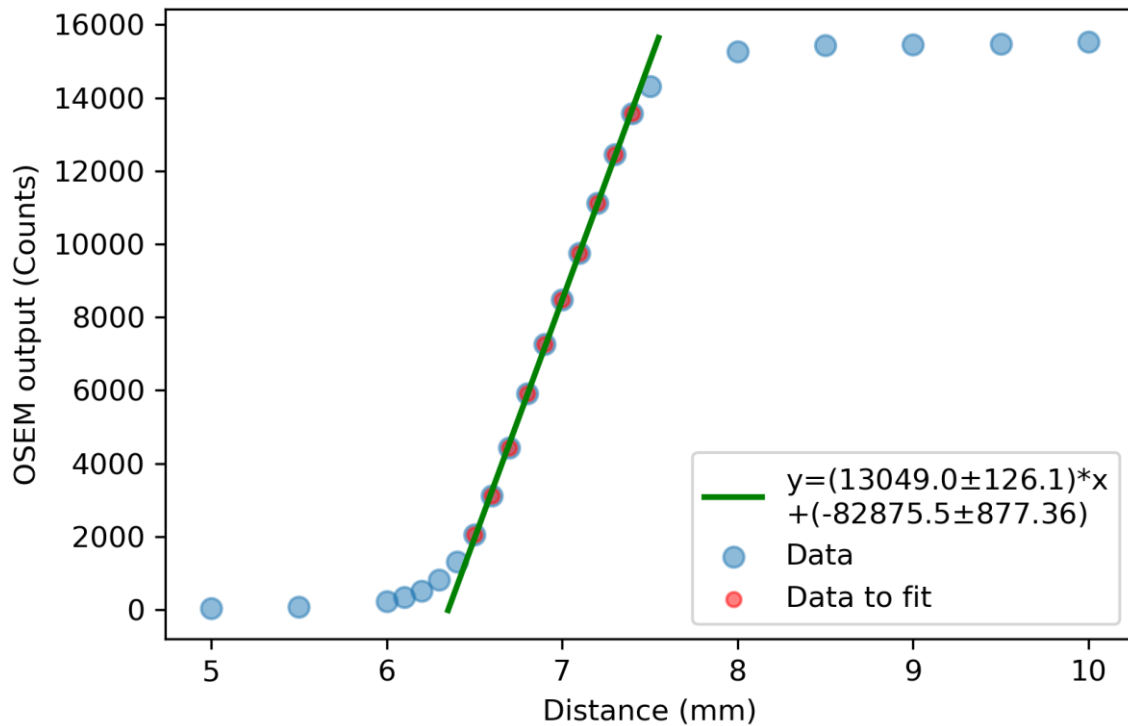
- The position sensor is a shadow sensor.
- It has a coil magnet-actuator.
- Mounted on IRM.
- 6 × OSEMs for 6 DoF: L, T, V, R, P and Y.



When the IM moves the flag changes the amount of light reaching the photodiode.

OSEM calibration and sensitivity

- Calibration factor: 2.89 mV/ μm
- Linear range: 0.9 mm

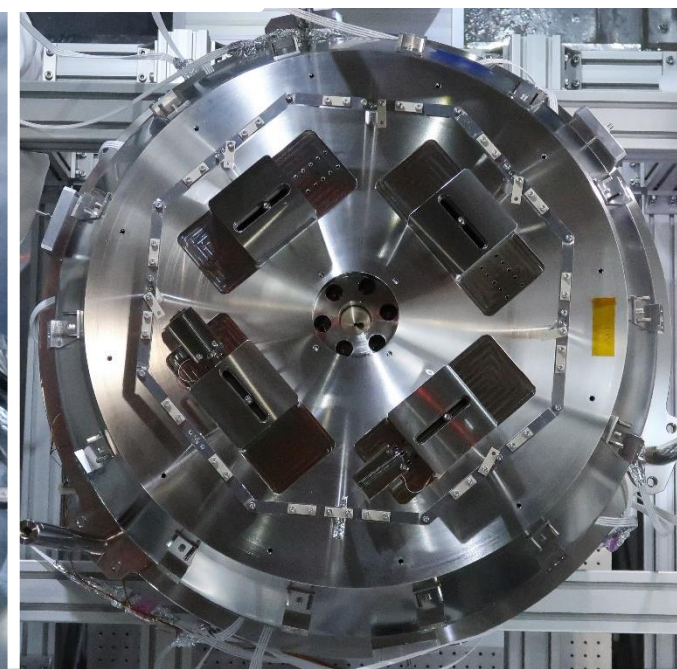
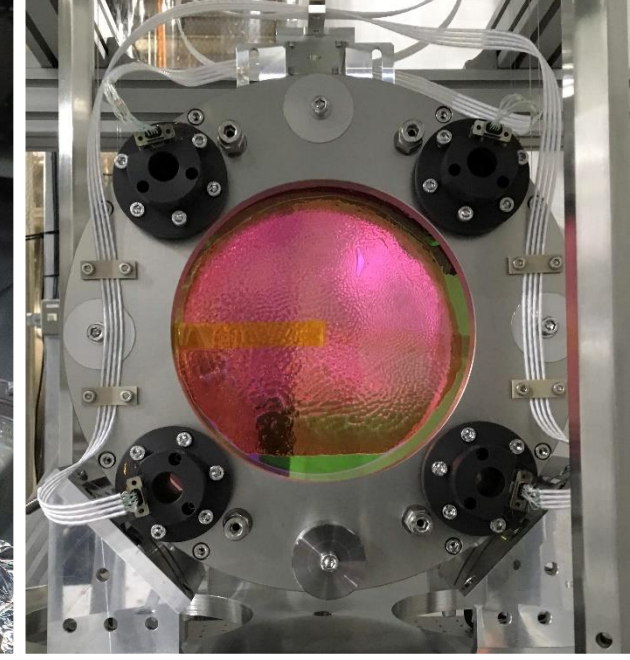
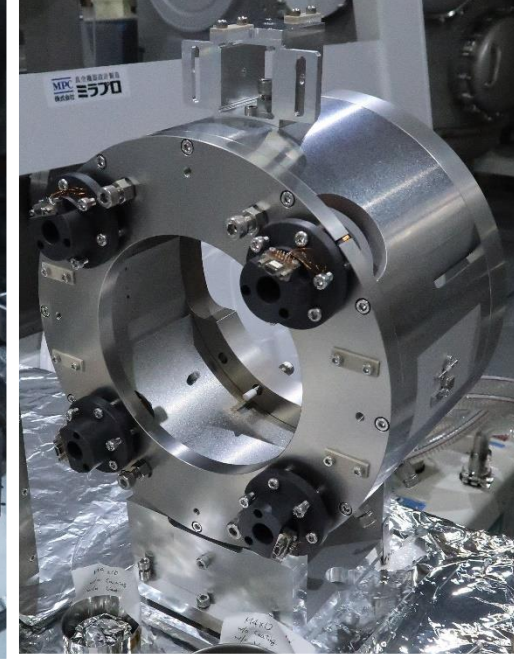
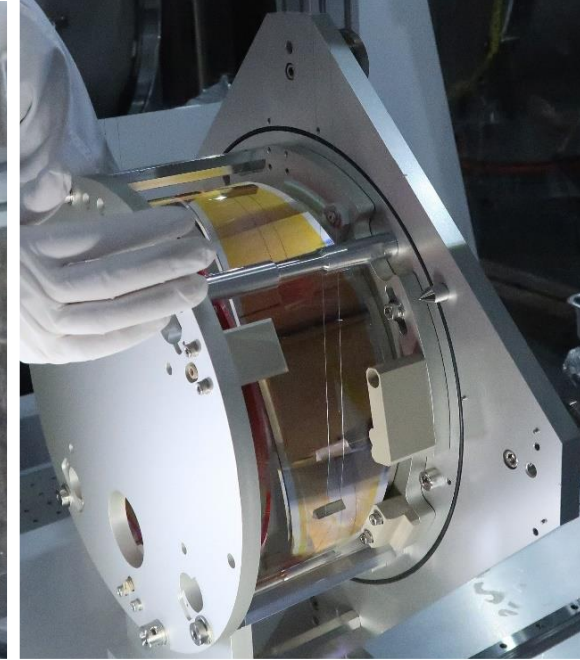
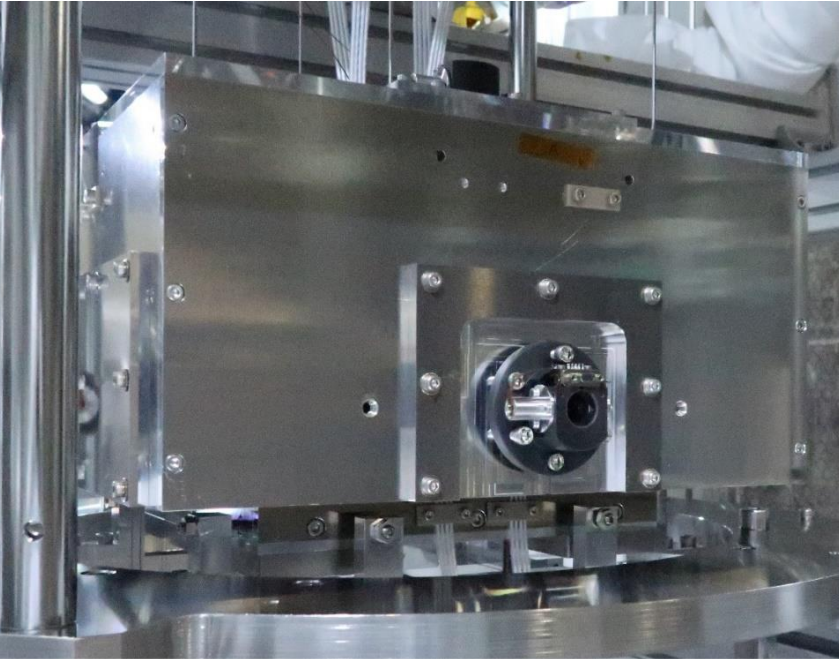


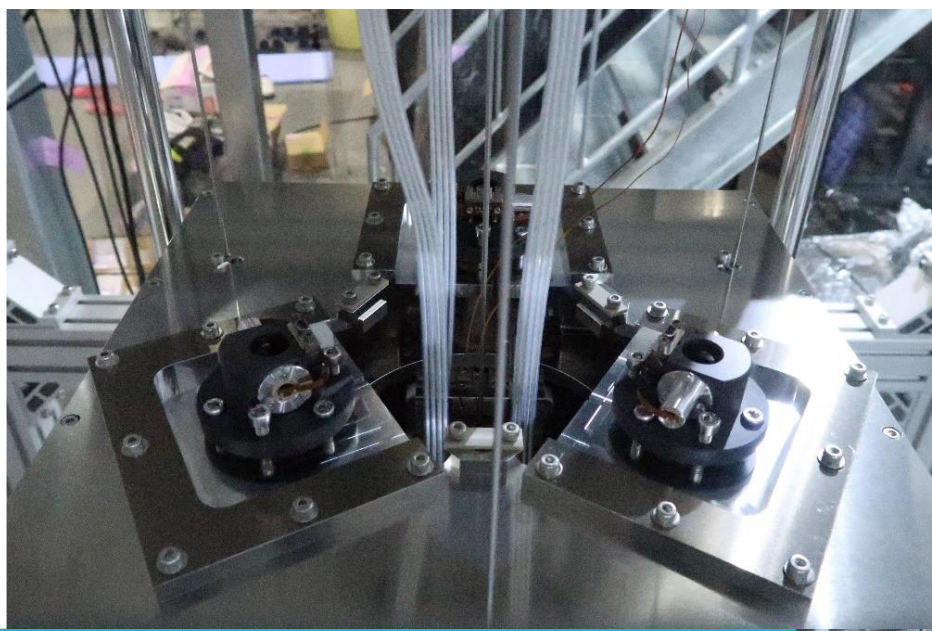
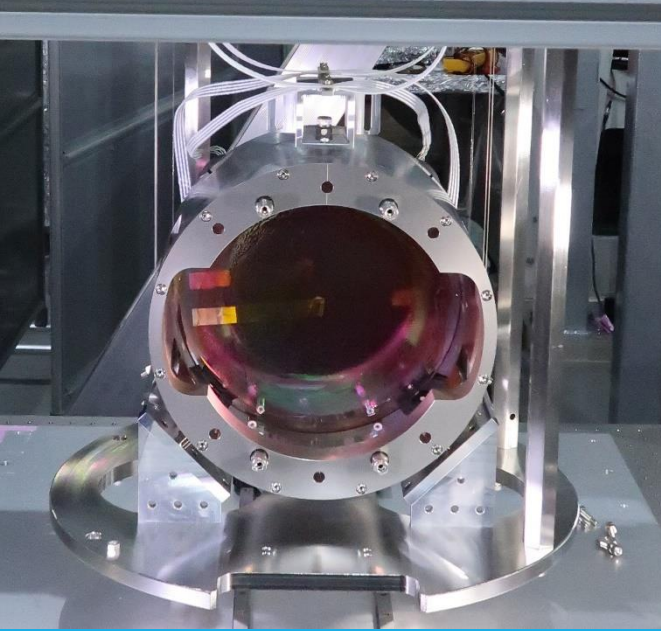
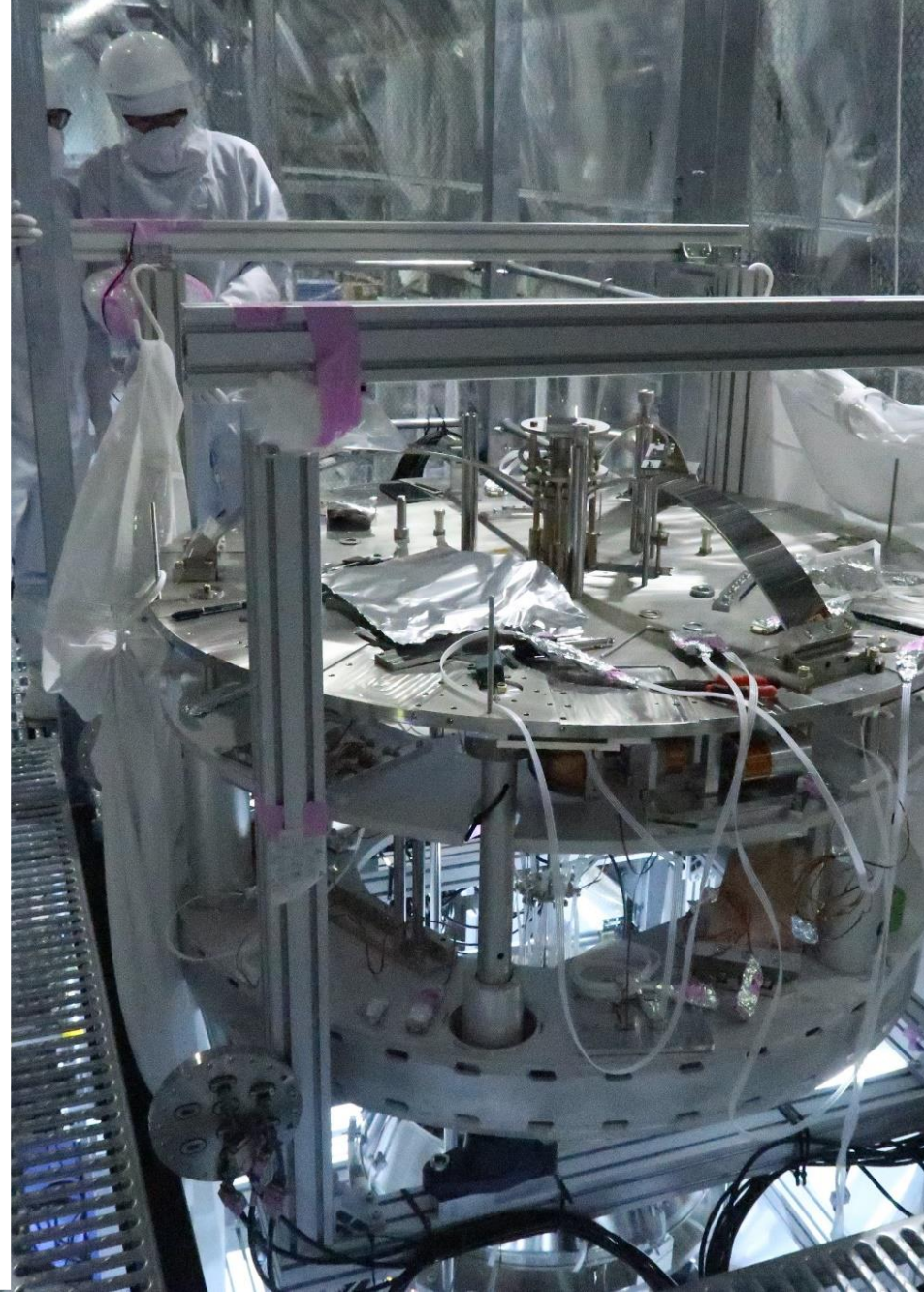
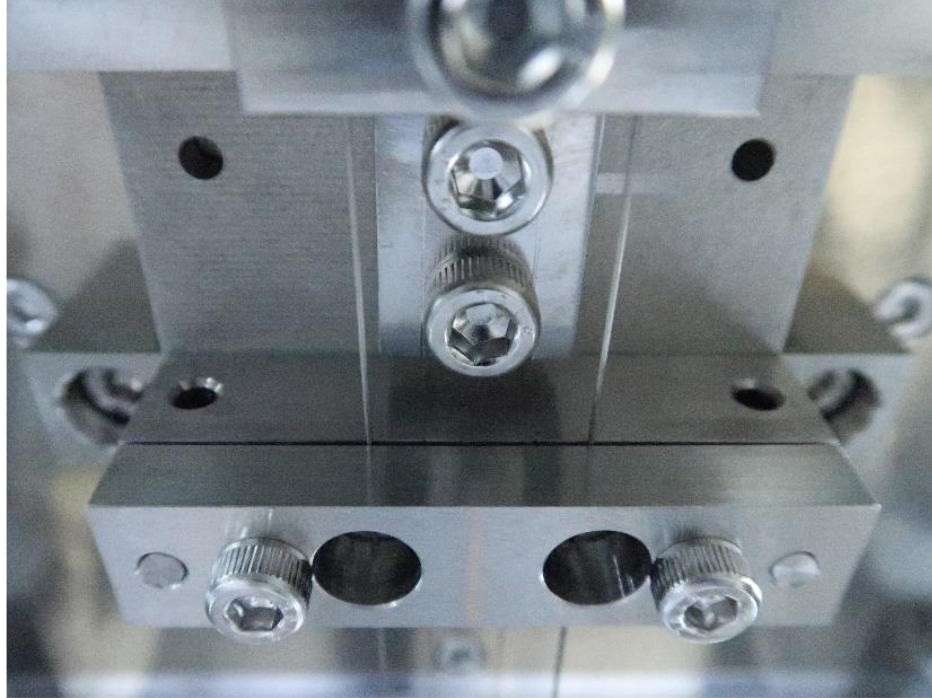
Measured by Panwei

A quick graphical tour to assembly

Just a few pictures



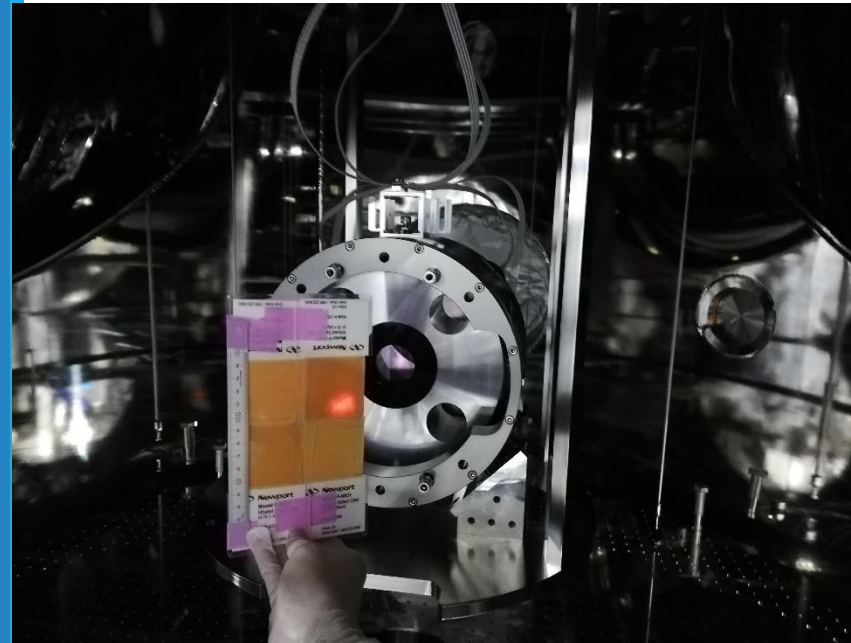




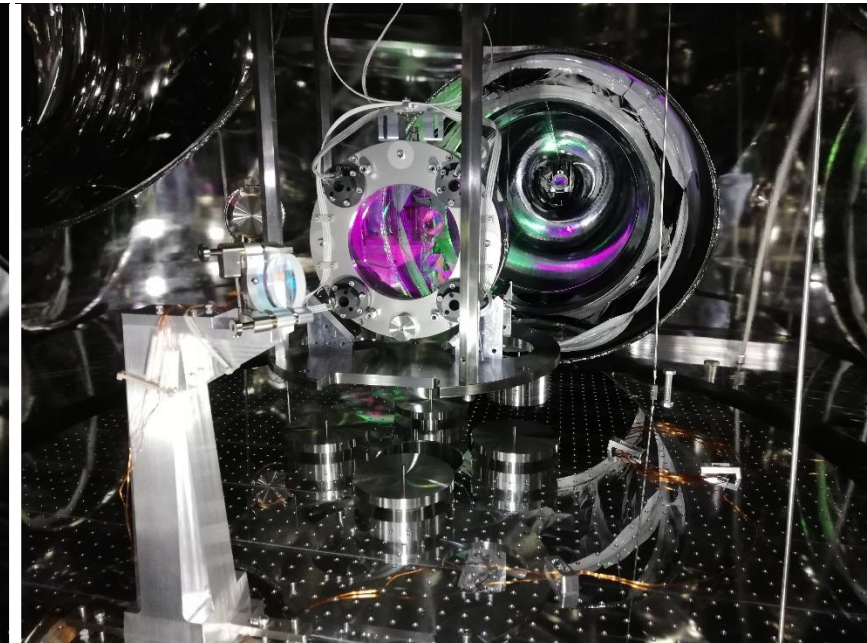
Some measurements, simulation and status.

- How does the system behave at low frequencies? **Enzo has an answer!**
- What does the suspension model predict within the **interferometer observation band** above 10 Hz?

SRM with interference pattern



SR2 with SR3 far away along the pipe



Tools for simulation

SUMCOM: free hanging suspension

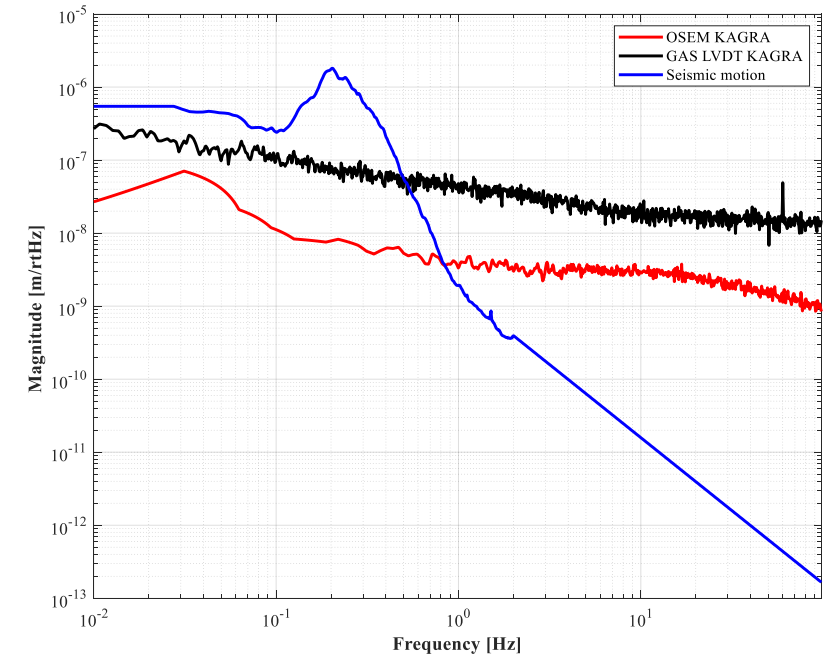
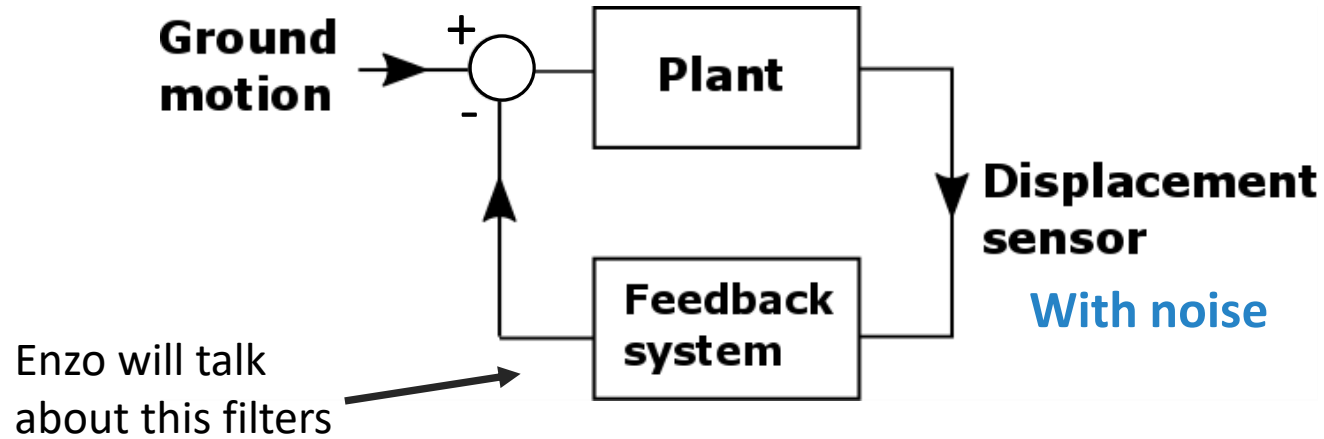
- Mathematica.
- Transfer function and list of resonant modes.
- It's capable of taking into account structural damping using complex numbers.
- Control system simulation has not being implemented.
- It provides a graphical representation of the resonant modes.

Control system simulation

- Matlab/Simulink.
- Transfer function and list of resonant modes.
- Only viscous damping is available.
- It's used to assess the sensor noise fed back into the system.
- Control filter design above 10 Hz.

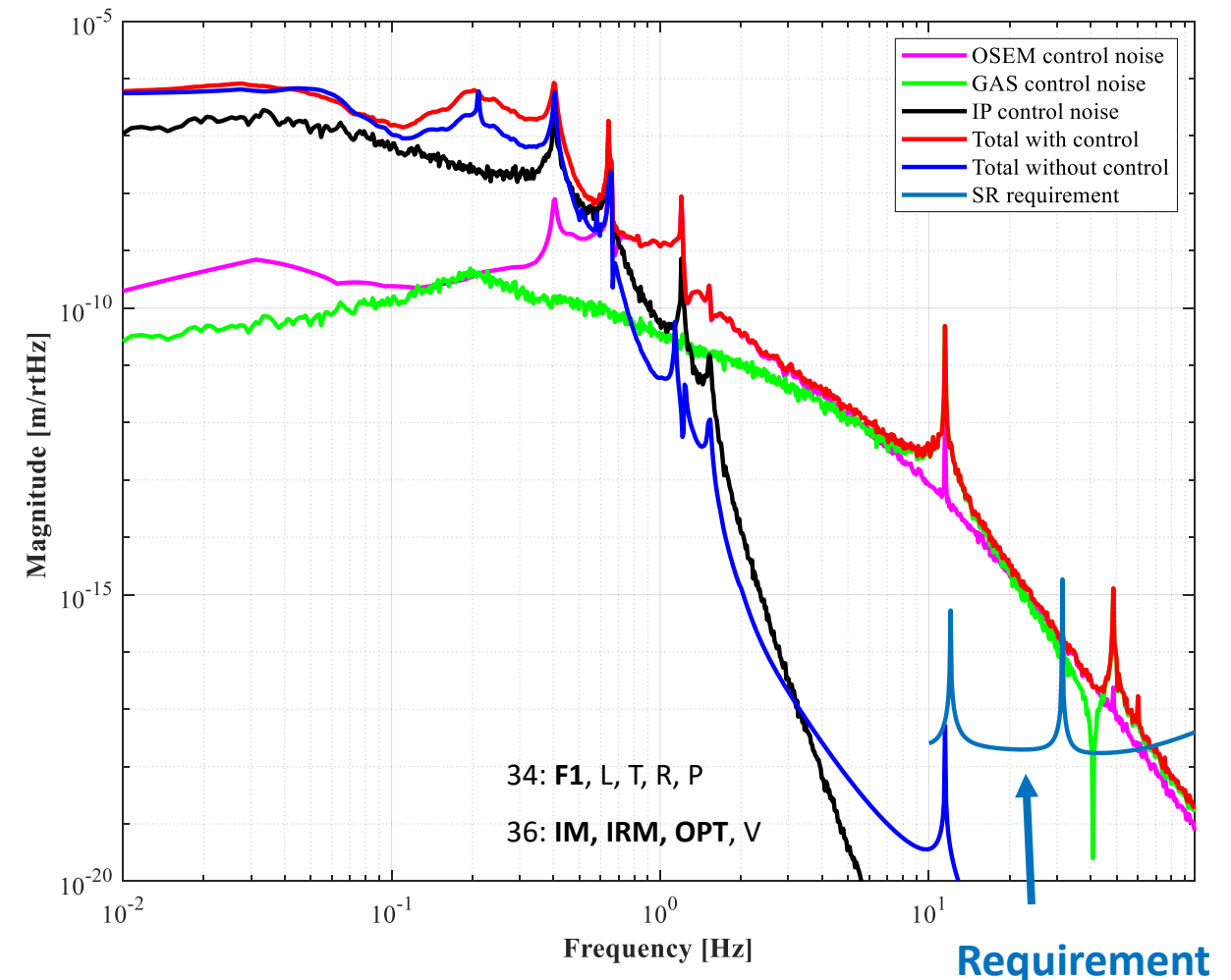
Software written by Takanori Sekiguchi

Noise in sensors and the control loop



Current status: residual motion within the observation band

- We have calculated the motion of the optic to be too large within the observation frequency band.
- The GAS LVDT noise fed back by the control loop is too high. **Control filters still have to be rolled-off** above resonant frequencies and below 10 Hz.
- Inertial damping not implemented yet.
- The calculation assumes 1% coupling from the vertical to the horizontal degree of freedom.
- The OSEMs are expected to be off during observation. Angular control will be transferred to the main interferometer which uses wavefront sensors.

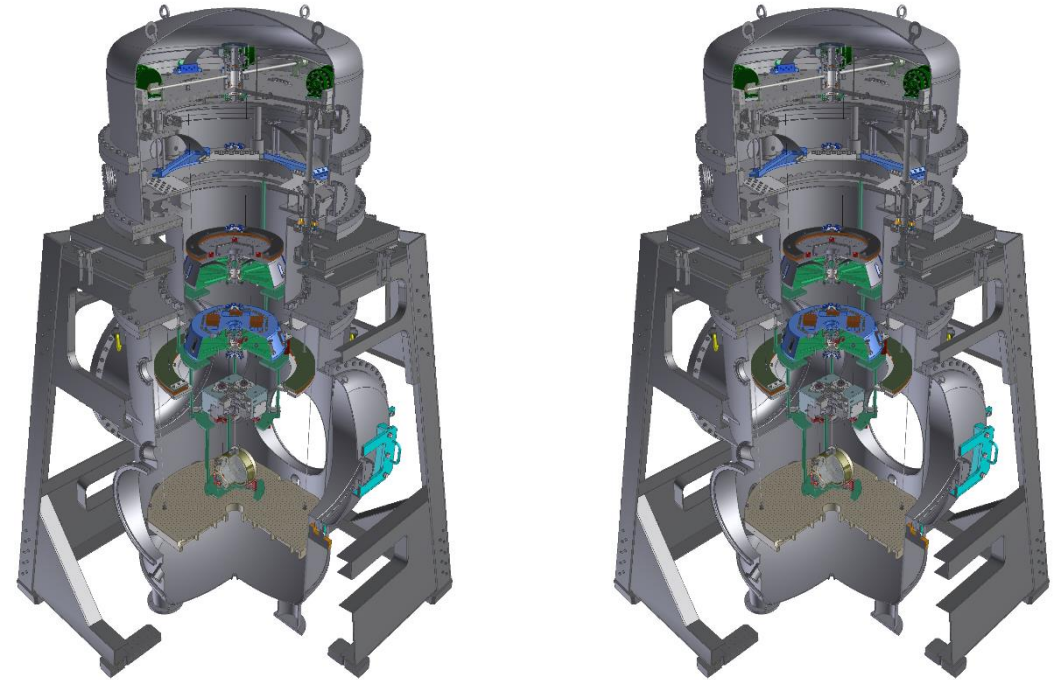


Immediate future work

- We will attempt to take advantage of the **common mode rejection** there may be among suspensions.
- Characterization within the interferometer observation band.

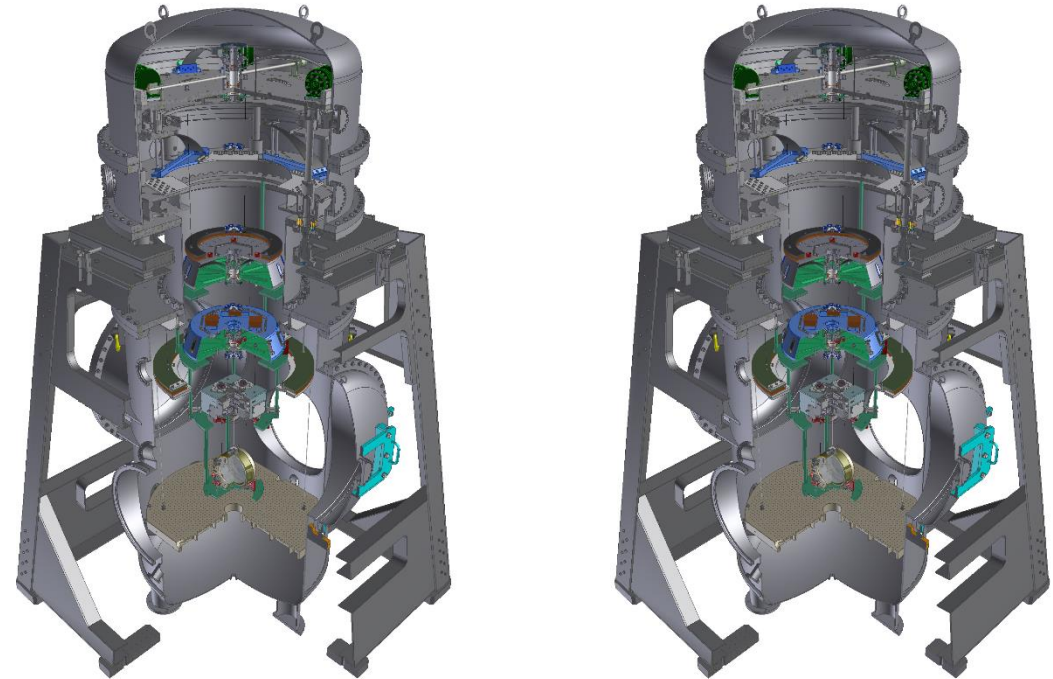
Common mode rejection (1)

- In general, the suspensions move in **dissimilar** ways.
- In principle, in order to keep the mirrors as still as possible **with respect to each other**, perturbations have to be **damped locally** at each suspension.



Common mode rejection (2)

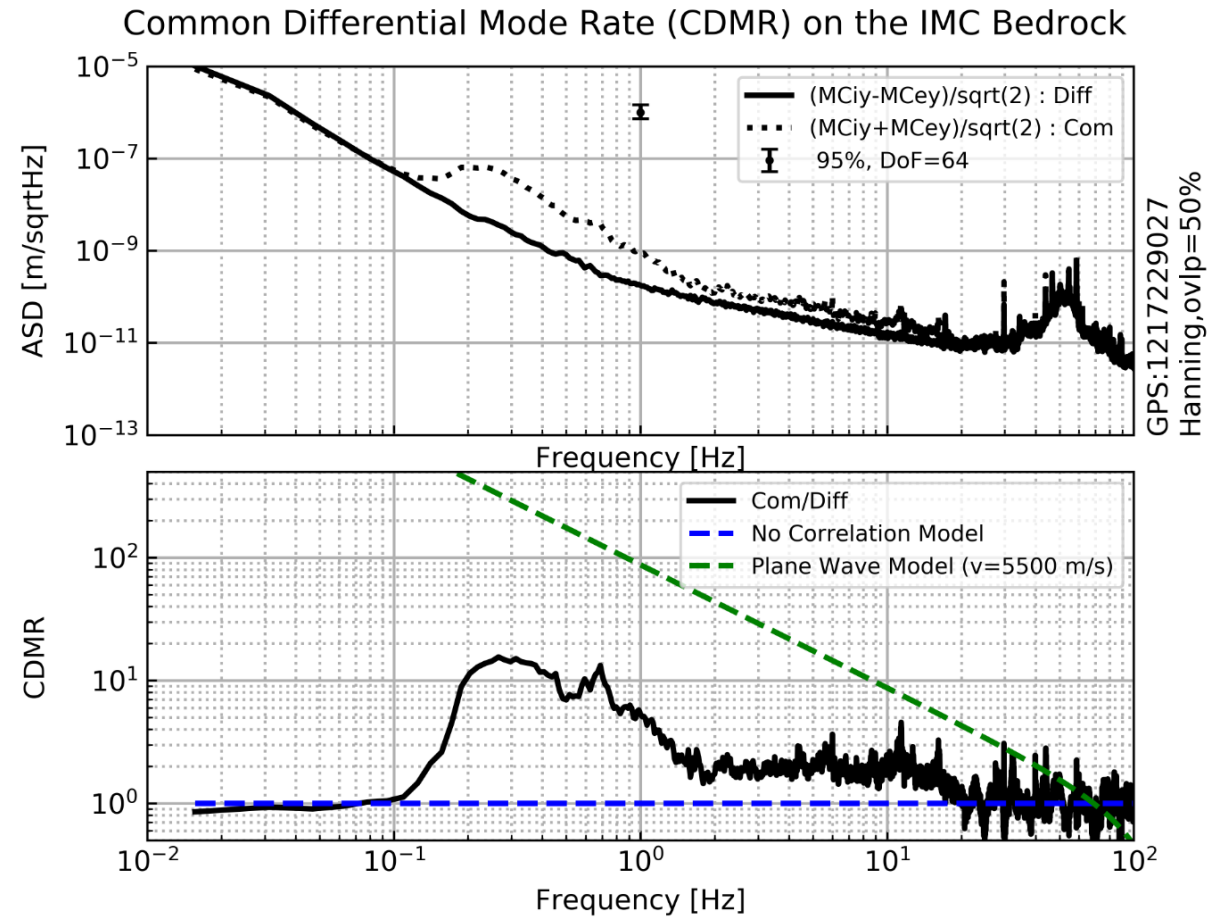
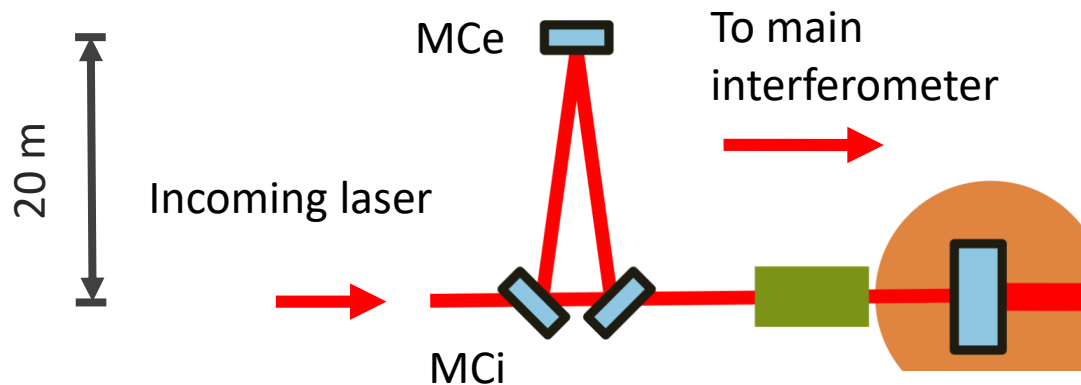
- Nevertheless, we found evidence that in the central room the **suspensions move together to a certain extent.**
- We would like to explore how to use this **common mode** movement in order to design a suitable control strategy.



Common mode rejection evidence

Common and differential seismic motion was measured in the **Input Mode Cleaner** area:

- Below 20 Hz down to almost 0.150 Hz the common mode is larger than the differential mode.
- A *very simple preliminary* model of the a plane wave traveling along the length of the IMC tunnel does not agree with the measurement.
- More work is necessary.

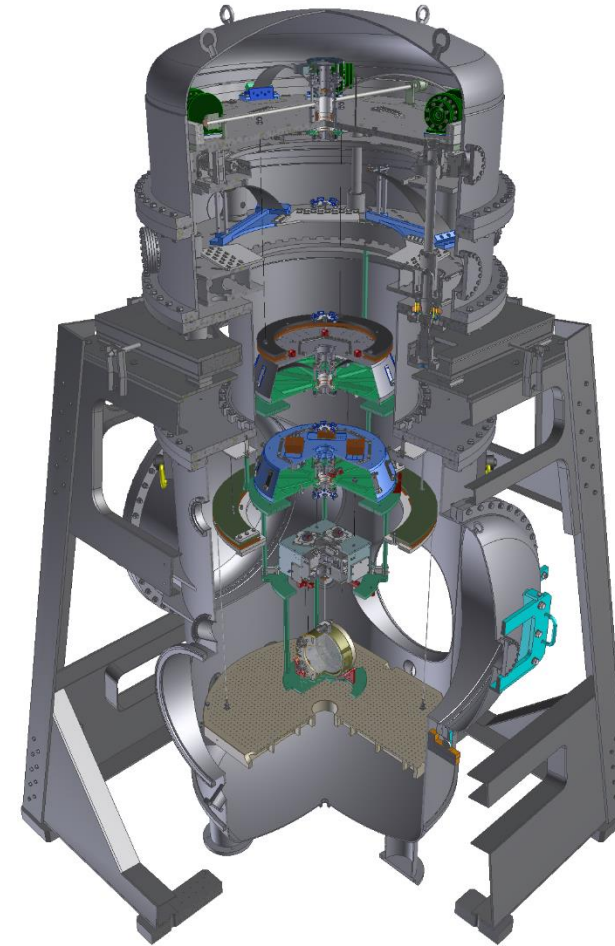


GPS:1217229027
Hanning,ovlp=50%

Measurement and calculation by Kousei Miyo

Dual recycling Michelson Interferometer

- We'll use the DRMI as a displacement sensor for characterization.
- Measure residual motion.
- Decide whether to use inertial damping or common-mode rejection.
- We'll use the back reflections of the input Test Masses.
- The PR cavity will be used for laser frequency stabilization.
- We aim to shake the IP and measure geophone output and interferometer output.

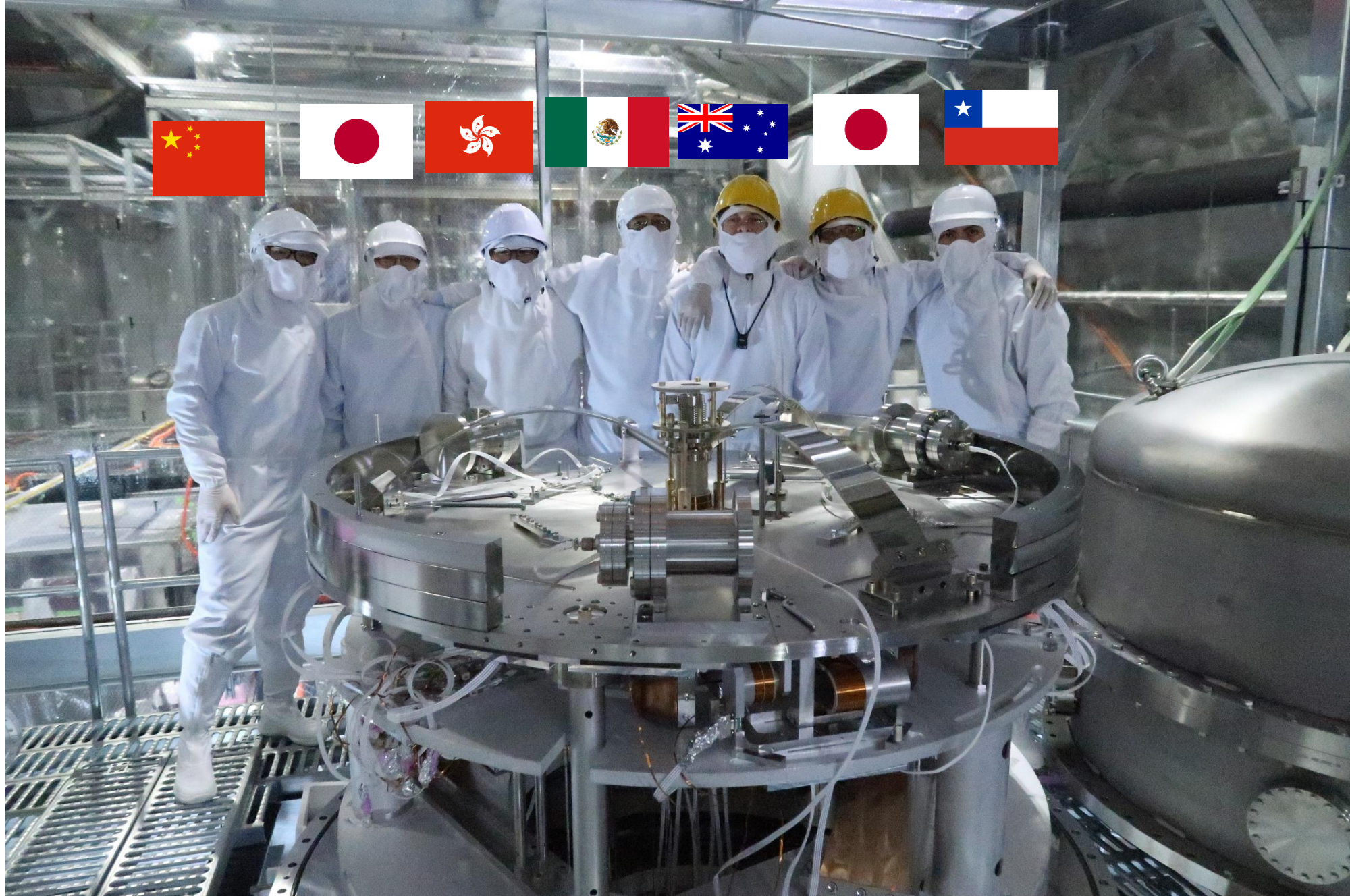


- We have built four Type B suspensions for the beam splitter and signal recycling mirrors.
 - Passive vibration isolation: IP and three GAS filters.
 - Active vibration isolation: LVDTs, OSEMS and coil-magnet actuators.
 - Payload comprises a marionette, the optic and their recoil masses.
- More work is required to meet the requirement of at 10 Hz, namely, to roll-off the GAS control filters.
- We aim to characterize the system by shaking the IP table and measuring transfer function from geophones to interferometer output.
- We want to explore ways of using common mode rejection in order to design a suitable control strategy.

KAGRA is an international collaboration

This version of the Type B team has members from:

- Australia
- Mexico
- Japan
- Chile
- Hong Kong
- China

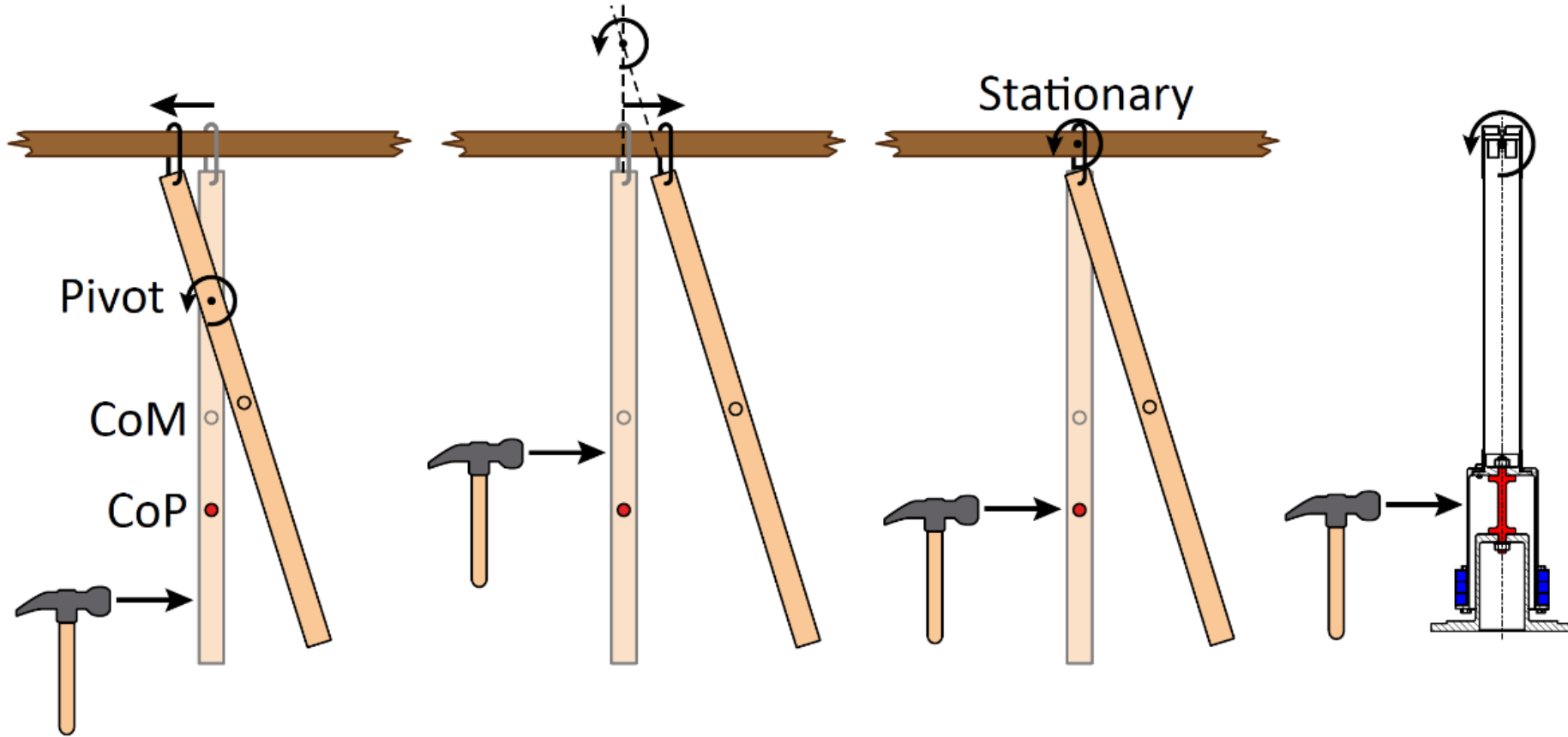


Temperature and GAS filters

	K	L	M	N	O
	Beam splitter				
	Filter	Frequency (Hz)	klog	Drift (mm/C°)	Total drift (mm)
	BF	0.448	3385	-0.314475604	-0.597503647
	F1	0.425	3376	-0.349433974	-0.66392455
	F0	0.209	3385	-1.444942001	-2.745389801

	E	F	G	H	I
	SRM				
	Filter	Frequency (Hz)	klog	Drift per degree (mm/C°)	Total drift (mm)
	BF	0.45	6886	-0.311686477	-0.592204306
	F1	0.38	6886	-0.437094955	-0.830480415
	F0	0.56	6886	-0.201264386	-0.382402334

Centre of percussion effect



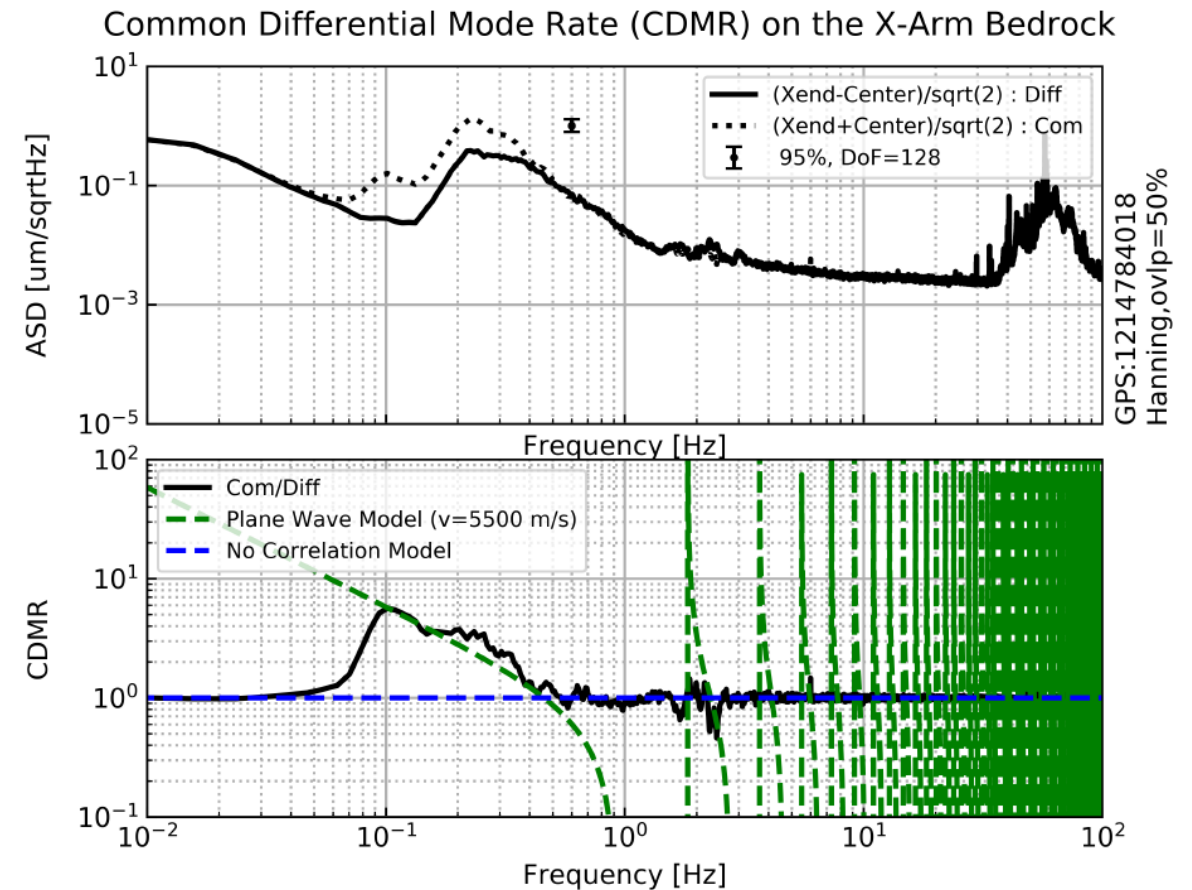
Drawing by Alexander Wanner

Common mode rejection evidence

The seismic noise common and differential modes were measured between the X end and the central room using seismometers:

- Below 0.4 Hz down to about 0.06 Hz the common mode is larger than the differential mode.
- A *very simple preliminary* model of the a plane p-wave traveling along the length of the X arm agrees with the measurement.
- More work is necessary.

Measurement and calculation by Kouseki Miyo



Inverted pendulum and top filter (1)

